PHILOSOPHICAL TRANSACTIONS OF THE ROYAL SOCIETY A MATHEMATICAL, PHYSICAL & ENGINEERING SCIENCES

A Model of Dislocation-Controlled Rheology for the Mantle

J. B. Minster and D. L. Anderson

Phil. Trans. R. Soc. Lond. A 1981 **299**, 319-356
doi: 10.1098/rsta.1981.0025

A MODEL OF DISLOCATION-CONTROLLED RHEOLOGY FOR THE MANTLE

BY J. B. MINSTER AND D. L. ANDERSON
Division of Geological and Planetary Sciences,
California Institute of Technology, Pasadena, California 91125, *U.S.A.*

(*Communicated by G. B. Whitham, F.R.S. – Received* 8 *April* 1980)

CONTENTS

Vol. 299. A 1449. 25 [Published 11 February 1981

The dislocation microstructure of mantle materials can account simultaneously for long-term steady-state creep, and for stress wave attenuation at seismic frequencies. The hypothesis that a single microstructural model explains the rheology for characteristic times ranging from 1 to 10^{10} seconds can be used to restrict the class of permissible rheological models for the mantle. We review steady-state dislocation damping models in order of increasing complexity, and reject those which do not satisfy laboratory data or geophysical constraints.

This elimination procedure leads us to consider an organized microstructure, in which most dislocations are found inside subgrain walls. The cells contain relatively few dislocation links. These are free to bow under small, i.e. seismic, stresses. The time constant of this mechanism is controlled either by the diffusion of kinks or of point defects bound to the dislocation line. The glide of intragrain dislocations explains the magnitude and frequency range of seismic attenuation. Steady-state creep is governed by recovery through climb and annihilation in cell walls. Under conditions of jog undersaturation, climb is controlled by jog formation in addition to self-diffusion, and the model requires a higher creep activation energy than for self-diffusion, in agreement with observations on olivine. Quantitative agreement with laboratory data is achieved if the density of cell-wall dislocations is one to two orders of magnitude higher than the density of intracell dislocations. Self-diffusion is probably controlled by silicon diffusion at low pressure and by oxygen diffusion at high pressure. The long-term tectonic stress is the dominant factor determining scale lengths; as a result, the total strength of the relaxation associated with bowing of intracell dislocation links is fixed by the geometry and is of the order of 10 %. This limits the width of the seismic absorption band to 2–3 decades in frequency for each mantle mineral. The actual position of the seismic absorption band is determined primarily as a result of a trade-off between temperature, pressure and tectonic stress.

This model provides a physical framework within which the quality factor Q and viscosity are related via the dislocation microstructure.

PHILOSOPHICAL TRANSACTIONS OF THE ROYAL SOCIETY A MATHEMATICAL, PHYSICAL & ENGINEERING SCIENCES

Notation

α	exponent for frequency dependent Q
b	Burgers vector
β_d	geometrical constant
c_j	jog concentration
C	normalization constant
d	climb distance for annihilation
D, D_0	diffusivity and pre-exponential diffusion constant
D_{0Q}	diffusion constant for attenuation
D_{0s}	diffusion constant for self-diffusion
$D(\tau)$	retardation spectrum
$\gamma(\omega)$	attenuation coefficient
Δ	relaxation strength
$E_m^* \leqslant E^* \leqslant E_M^*$	activation energy and range
E_Q^*	activation energy for attenuation
E_s^*	activation energy for self-diffusion
E_j	jog formation energy
E_k	kink formation energy
ΔE^*	difference between bulk and core diffusion
$\epsilon, \dot{\epsilon}$	strain and strain rate
$J(t)$	compliance response
J_u	unrelaxed compliance
J_r	relaxed compliance
δJ	compliance defect
K, K_m, K_s	microstructural scaling constants
k	Boltzmann constant
$k(\omega)$	complex wavenumber
$l, \bar{l}$	dislocation link length, and average
$L, \bar{L}$	subgrain size, and average
l_c	critical length for multiplication
λ	scale length for dislocation drag mechanism
λ_v	scale length for vacancy diffusion
Λ	mean free path of dislocations
μ	rigidity
n_w	number of lattice spacings between cell wall dislocations
ω	frequency
Ω	atomic volume
Ω_v	vacancy volume
$p(l), p(E^*)$	probability distributions
P	pressure
$\Psi(t)$	creep function
$Q(\omega)$	quality factor
R	gas constant
R_c	radius of curvature of dislocation line

PHILOSOPHICAL TRANSACTIONS OF THE ROYAL SOCIETY A MATHEMATICAL, PHYSICAL & ENGINEERING SCIENCES

r_w	dislocation spacing in cell walls
r_1, r_2	inner and outer cut-off radii for vacancy diffusion
ρ	total (smeared) dislocation density
ρ_m	density of mobile dislocations
ρ_w	density of dislocations composing cell boundaries
σ_s	seismic (transient) stress
σ_t	tectonic (steady state) stress
T	temperature
t_μ	time for multiplication
τ	retardation time
τ_0	pre-exponential retardation time
τ_m, τ_M	limits of retardation spectrum
$\hat{\tau}$	Maxwell time
V, V_D	dislocation migration (drift) velocity
$V_p(\omega)$	phase velocity
V_u, V_r	unrelaxed and relaxed phase velocities
V^*	activation volume
$\bar{z}$	mean free path of vacancy along dislocation core

Subscripts

N.H.	Nabarro–Herring diffusion
i.g.	intragrain recovery mechanism
p.u.	dislocation pile-up mechanism
c.w.	cell-wall recovery mechanism
sq	σ^2 creep law

Introduction

It is probable that steady-state creep in the mantle is controlled by dislocation climb (Weertman 1970, 1975; Goetze & Brace 1972; Green & Radcliffe 1972; Goetze & Kohlstedt 1973) and is therefore limited by the slow process of self-diffusion and, possibly, jog nucleation. On the other hand, dislocation motion at short times and under very low stress is probably due to glide and is rate-limited by faster diffusional processes involving small point defects or kinks (see, for example, Simpson & Sosin 1972). This has led Gueguen & Mercier (1973) and Anderson & Minster (1980*a*) to propose diffusion-controlled dislocation bowing as an attenuation mechanism for seismic waves in the mantle. There is therefore a possible close connection between seismic attenuation and viscosity via the dislocation structure of the mantle.

In this paper we develop a simplified physical model which allows us to bridge the vastly different time scales and strains involved in steady-state creep and anelastic behaviour. The fundamental assumption is that the microstructure of mantle grains is controlled by long-term processes and is therefore statistically time invariant, and that mobile dislocation links are free to bow by glide under small transient stresses. The long-term, large strain deformation is controlled by climb, and therefore by self-diffusion and jog formation. The small anelastic strain associated with bowing of mobile dislocation links leads to stress relaxation and consequently to attenuation of stress waves. Although greatly simplified, the formalism is quite general and can accommodate a distribution of grain sizes, dislocation link lengths and acti-

vation energies. The detailed analysis will be made for a physically plausible and geophysically interesting family of such distributions. The necessary scaling relations are given in §1.

We then develop a formal theory of attenuation by diffusion-controlled dislocation bowing, and provide the necessary results to analyse absorption bands with a mild frequency dependence of Q. In §3 we present a sequence of creep models of increasing complexity, and recast all results in terms of Maxwell characteristic times. This permits us to test the various models against quantitative observational constraints as well as to impose the necessary constraints for self-consistency. This is done in §4 for creep models as well as for attenuation models. We show that quantitative agreement with laboratory data and geophysical observations can be achieved simultaneously for both aspects of the rheology if the microstructure presents a fairly high degree of organization. The preferred creep model is a generalization of Gittus's (1976*a*) model. The width of the absorption band is probably associated with a distribution of activation energies and/or dislocation link lengths.

1. Scaling laws

Although there is abundant evidence that mantle minerals contain many dislocations (see, for example, Raleigh & Kirby 1970; Green & Radcliffe 1972; Goetze & Kohlstedt 1973), the actual microstructure under mantle conditions is uncertain. Plausible assumptions can be made, however, since the bulk of mantle material has remained under quasi-constant low stress (1–10^2 bar†) over long times (more than 10^6 years). In view of the high temperatures and pressures, we can assume that the dislocation microstructure of mantle minerals *in situ* is that pertinent to high-temperature steady-state creep.

The substructural characteristics associated with high-temperature steady-state creep have been observed for a wide variety of materials. Summaries of the most significant properties show that they are remarkably similar from material to material (see, for example, Mukherjee *et al.* 1969; Poirier 1976; Takeuchi & Argon 1976*a*; Durham *et al.* 1977). By comparison with laboratory results, and in view of the supporting theories of Gittus (1976*a*, *b*), we shall assume that most dislocations in the mantle are associated with cell walls of subgrains, and that the subgrains contain only a few dislocations, with no tangles or pile-ups. We shall further assume that these few free dislocations may be strongly pinned at isolated points, and that the segments between pinners can bow out under low stress. Under larger stress, multiplication may take place, either by glide (Frank–Read sources) or climb (Bardeen–Herring sources).

The problem of superposing a low-level transient (seismic) stress on a much larger steady (tectonic) stress is complex. Because of the very different time scales involved, the problems can be decoupled to first order, and we shall assume that the transient is actually superposed on a static, 'equilibrium' configuration of internal stress.

Further specification and simplification of the model can be achieved by use of the following empirical scaling laws (see, for example, Mukherjee *et al.* 1969; Takeuchi & Argon 1976*a*):

(i) The average subgrain size is inversely proportional to the (tectonic) stress;

$$\bar{L}/b \propto \mu/\sigma_t, \tag{1}$$

where b is the Burgers vector and μ the rigidity.

† *Note on units.* The authors have particularly requested that units of measurement such as bar, calorie and poise be retained (rather than have the values expressed in SI units) to facilitate comparison with the many publications cited from solid state, metallurgical, petrological and geophysical literature that predate 1975 and use the CGS system.

Conversion factors: bar = 10^5 Pa; calorie = cal = 4.184 J; poise = 10^{-1} Pa s.

(ii) The dislocation density within subgrains is proportional to the square of stress:

$$b^2\rho_m \propto (\sigma_t/\mu)^2. \tag{2}$$

Here we have identified intragrain dislocations with the mobile dislocations of density ρ_m. Comparison of these two scaling laws leads to

$$b^2\rho_m \approx K_m^2(b/\bar{L})^2. \tag{3}$$

The observations of Durham *et al.* (1977) on laboratory-deformed olivine lead to a proportionality constant K_m of the order of 10, although this value is quite uncertain. Since the volume of subgrains is proportional to $\bar{L}^3$, this implies that the length of dislocation line per cell is proportional to the cell dimension $\bar{L}$. We may assume that this statistical scaling law holds locally, in the sense that it holds in a neighbourhood which is very large compared with the cell size but very small compared with the averaging length of a seismic wave.

If ρ is the total dislocation density, then we may write

$$\rho = \rho_m + \rho_w, \tag{4}$$

where ρ_w is the density of dislocations composing cell walls. For materials showing a strong degree of organization, ρ_w may be over an order of magnitude greater than ρ_m (see, for example, Takeuchi & Argon (1976*a*)) and is thus is a good approximation to the 'smeared' dislocation density, in the sense of Holt (1970) and Gittus (1976*a*, *b*). On the basis of theoretical and observational considerations, these authors argue that a relation similar to (3) holds for the smeared density, in the form

$$b^2\rho \approx K^2(b/\bar{L})^2. \tag{5}$$

Observations on metals point to values of K ranging from 10 to 20, but higher values may be expected theoretically for materials with a higher Peierls energy (Gittus 1976*a*, *b*). Consistency between the three equations (3)–(5) requires that ρ_m and ρ_w scale with grain size, and hence with stress in a similar way. Further, ρ_w is an order of magnitude larger than ρ_m if K is only three times greater than K_m.

Although most of the preceding considerations are based on observational evidence on metals, the observations of Durham & Goetze (1977) and Durham *et al.* (1977) indicate that olivine is no exception. Of course, detailed description of the microstructure involves many complications, so that the present model must be taken as an idealization. Our purpose is to test some of its consequences.

2. Diffusion-controlled dislocation damping

(*a*) *Retardation spectrum*

The most commonly – and most successfully – used model of dislocation damping is the classical Koehler–Granato–Lücke model (Koehler 1952; Granato & Lücke 1956). This is a string model for a dislocation strongly pinned at both ends, and we use it as a starting point. A recent treatment of the problem at low frequency, where inertial effects can be neglected, is given by Simpson & Sosin (1972).

We may write the force-balance equation for the string model of the dislocation line in the following form:

$$\sigma_s b - \mu b^2/2R_c - VkT/\lambda D = 0. \tag{6}$$

Here σ_s is the applied (seismic) stress, R_c the radius of curvature, and V the migration velocity (figure 1). λ and D are a scale length and a diffusion coefficient which are characteristic of the particular viscous drag mechanism considered. Since we treat the problem as the superposition of a transient (seismic) stress on an equilibrium state, R_c and V take the values which correspond to equilibrium with σ_s. For small bow-out (6) reduces to a diffusion equation, and solutions have been derived by Friedel *et al.* (1955), Weertmann (1955), Schoeck (1963), and numerous other authors.

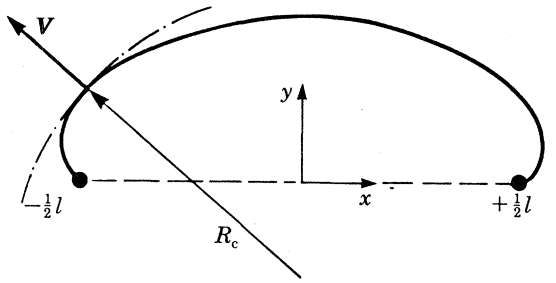

FIGURE 1. Sketch of a bowing dislocation of length l strongly pinned at both ends. V is the migration velocity; R_c is the radius of curvature.

For a link of length l, strongly pinned at both ends, the anelastic strain due to bow-out is given by

$$\epsilon(t) = \epsilon(\infty)\,[1-\exp(-t/\tau)], \tag{7}$$

which is the classical result for a standard linear solid, where the retardation time is

$$\tau = 2l^2kT/\pi^2\mu b^2\lambda D. \tag{8}$$

If we introduce the steady-state drift velocity V_D of an infinite dislocation line under the applied stress σ_s,

$$\tau = \frac{1}{\pi^2}\frac{\sigma_s}{\mu}\frac{l^2}{bV_D}, \tag{9}$$

which is also of the general form

$$\left.\begin{aligned}\tau &= \tau_0 \exp(E_Q^*/RT),\\ \tau_0 &= A(T)l^2/D_{0Q}.\end{aligned}\right\} \tag{10}$$

Here E_Q^* is the activation energy for this attenuation mechanism, and D_{0Q} is the pre-exponential diffusivity factor for the controlling diffusing species.

A distribution of retardation times can be achieved through a spectrum of pre-exponential factors τ_0 and/or a spectrum of activation energies E_Q^*. It is well known (see, for example, Nowick & Berry 1972) that a localized distribution of retardation times, with a spectrum decaying rapidly away from a dominant value, can be replaced for most purposes by an effective, single mechanism. In such cases, the essential characteristics of the medium do not differ drastically from those of a standard linear solid.

It is more useful, for our purposes, to allow for the possibility that a broad spectrum of retardation times is available. We have suggested previously (Anderson & Minster 1980*a*; Minster & Anderson 1980) a normalized density of the form

$$D(\tau) = \frac{\alpha}{\tau_M^\alpha - \tau_m^\alpha}\frac{1}{\tau^{1-\alpha}}\,H(\tau-\tau_m)\,H(\tau_M-\tau). \tag{11}$$

Among the many possible physical models that entail the distribution (11) we shall consider two extreme cases:

(i) A distribution of lengths with probability density

$$p(l) = C_l\, l^{2\alpha-4}, \quad l_{\mathrm{m}} < l < l_{\mathrm{M}}, \tag{12}$$

where C_l is the normalization factor.

(ii) A distribution of activation energies with probability density

$$p(E_Q^*) = C_E \exp(\alpha E_Q^*), \quad E_{\mathrm{m}}^* < E_Q^* < E_{\mathrm{M}}^*, \tag{13}$$

where C_E is again a normalization factor.

The general case clearly consists of a simultaneous distribution of lengths and activation energies. In his discussion of the problem, Macdonald (1963) also considers juxtaposed intervals in τ with different values of α.

As we shall see shortly, the non-local character of the absorption band associated with the spectrum (11) is only significant for small values of α. The richest variety of rheological behaviour is observed for α in the range $[-1, 1]$; in the remainder of this paper, we confine our attention to this range. Note, however, that the limit $\alpha \to 0$ must be taken with some care, and results for this case will be given separately.

The cut-offs τ_{m} and τ_{M} are taken here as phenomenological parameters to be constrained by the physical model. Since the actual behaviour of the spectrum outside the range $[\tau_{\mathrm{m}}, \tau_{\mathrm{M}}]$ is immaterial for our purposes, as long as $D(\tau)$ decays rapidly away from this range, we have assumed sharp cut-offs. Localized spectra can be conveniently simulated by taking a narrow range, $\tau_{\mathrm{m}} \approx \tau_{\mathrm{M}}$, irrespective of α.

Let J_{u} be the unrelaxed compliance of the material, and δJ be the compliance defect. The compliance response is then

$$J(t) = J_{\mathrm{u}} + \delta J \psi(t) = J_{\mathrm{u}}[1 + \Delta\psi(t)]. \tag{14}$$

Here $\psi(t)$ is the normalized creep function and Δ the relaxation strength. The medium is anelastic, that is, it undergoes time-dependent, but linear and recoverable, strain response to an applied stress (Nowick & Berry 1972; Minster 1980). The complete anelastic behaviour of the material under low stress can be described in terms of Δ and ψ.

(*b*) *Relaxation strength*

The compliance defect δJ depends on the total area swept by mobile dislocations as they bow out, as $t \to \infty$. The calculation is a classical one (see, for example, Friedel *et al.* 1955) and yields

$$\Delta = \beta_{\mathrm{d}} \frac{\rho_{\mathrm{m}}}{\bar{l}} \int_0^\infty l^3 p(l)\, \mathrm{d}l. \tag{15}$$

Here ρ_{m} is the density of mobile dislocations, $p(l)$ the density function of the link length distribution, and $\bar{l}$ the average link length. β_{d} is a geometrical factor which depends on the orientation and geometrical arrangement of the dislocations. For edge dislocations which may only glide, and are all optimally oriented, $\beta_{\mathrm{d}} \approx \frac{1}{6}$. If they are randomly oriented β_{d} drops to $1/6\sqrt{5}$. If they are allowed to bow by climb as well as glide, $\beta_{\mathrm{d}} \approx \frac{1}{6\sqrt{5}}\,\frac{\sqrt{7}}{6\sqrt{15}}$.

Actually, the averaging should only take place over the possible orientations of the glide planes (Friedel *et al.* 1955; Simpson & Sosin 1972). For our purposes, approximate estimates are sufficient. Evaluation of (15) leads to the following results:

(i) *Case of a distribution of activation energies*

$$\Delta \approx \beta_d \rho_m \bar{l}^2. \tag{16}$$

It may be noted that this result is the correct one whenever the distribution of lengths is highly localized. Whenever the separation of mobile dislocations is comparable to the length $\bar{l}$ (for example, Frank network), the relaxation strength is about 8 % for glide, and 11 % if climb is permitted as well.

(ii) *Case of a broad distribution of lengths, $l_m \ll l_M$*

We find in this case if α is small

$$\bar{l} \approx [(3-2\alpha)/(2-2\alpha)]\, l_m, \tag{17}$$

and we may distinguish three cases, according to the sign of α:

$$\alpha < 0, \quad \Delta \approx -4[(1-\alpha)^3/\alpha(3-2\alpha)^2]\, \beta_d \rho_m \bar{l}^2; \tag{18}$$

$$\alpha = 0, \quad \Delta \approx \tfrac{8}{9} \ln (l_M/l_m)\, \beta_d \rho_m \bar{l}^2; \tag{19}$$

$$\alpha > 0, \quad \Delta \approx \frac{4(1-\alpha)^3}{\alpha(3-2\alpha)^2} \left(\frac{l_M}{l_m}\right)^{2\alpha} \beta_d \rho_m \bar{l}^2. \tag{20}$$

Comparison with (12) and (17) indicates that the relaxation strength is dominated by the more numerous shorter links if α is small, and that it increases rapidly with α. This is in agreement with expectation since an increase in α leads to relatively more abundant long dislocations. Note that in equations (16)–(20) we can use the scaling law (3) in the form

$$\rho_m \bar{l}^2 = (K_m \bar{l}/\bar{L})^2, \tag{21}$$

which illustrates more precisely the effect of the microstructure. If the link length scales linearly with subgrain size, then a spread in the distribution of lengths tends to increase Δ towards values greater than the 10 % predicted by (16). If the link length $\bar{l}$ does not increase with $\bar{L}$, then the material tends to be underpopulated in mobile dislocations and the modulus defect is rather small.

(c) *Creep function*

The normalized creep function is given by

$$\psi(t) = \int_0^\infty (1 - e^{-t/\tau})\, D(\tau)\, d\tau. \tag{22}$$

With the density (11), evaluation of the integral yields

$$\psi(t) = 1 - \frac{\alpha t^\alpha}{\tau_M^\alpha - \tau_m^\alpha} \left[\Gamma\left(-\alpha, \frac{t}{\tau_M}\right) - \Gamma\left(-\alpha, \frac{t}{\tau_m}\right)\right], \tag{23}$$

where Γ is the incomplete Γ-function. This expression possesses a proper limit as $\alpha \to 0$, which can be expressed in terms of exponential integral functions:

$$\psi_{\alpha \to 0}(t) = 1 - \frac{1}{\ln (\tau_M/\tau_m)} \left[\mathrm{Ei}\left(-\frac{t}{\tau_m}\right) - \mathrm{Ei}\left(-\frac{t}{\tau_M}\right)\right]. \tag{24}$$

In the limit of a narrow spectrum ($\tau_m \approx \tau_M$), we get the case of a standard linear solid, which does not require elaboration. In the case of a broad spectrum ($\tau_m \ll \tau_M$), the creep history is best characterized in terms of three successive régimes.

(i) *Short-time régime*, $t \ll \tau_m$

For such short times, none of the dislocation segments has relaxed. We find:

$$\alpha < 0, \quad \psi(t) \sim \frac{-\alpha}{1-\alpha} \frac{t}{\tau_m}; \tag{25}$$

$$\alpha = 0, \quad \psi(t) \sim \frac{1}{\ln(\tau_M/\tau_m)} \frac{t}{\tau_m}; \tag{26}$$

$$\alpha > 0, \quad \psi(t) \sim \frac{\alpha}{1-\alpha} \left(\frac{\tau_m}{\tau_M}\right)^{\alpha} \frac{t}{\tau_m}. \tag{27}$$

This linear time-dependence implies Newtonian behaviour for small time. It is of interest that the normalized creep function ψ depends on the width of the spectrum in (26) and (27), but does not in (25), for which the density of long retardation times is much smaller. If we consider the combination $\Delta\psi$, this remains true in the case of a distribution of activation energies (equation (16)). On the other hand, combination of (18)–(20), and (25)–(27) show that, irrespective of α, $\Delta\psi$ depends only on l_m for small times if the spectrum is due to a length distribution. This last result could have been anticipated since only the shorter links can react on this time scale.

(ii) *Transitional régime*, $\tau_m \ll t \ll \tau_M$

During this interval, more and more dislocation links reach their final equilibrium position. As a result we expect this régime to be one of strain hardening. The dominant terms are, according to the sign of α:

$$\alpha < 0, \quad \psi(t) \sim 1 - \Gamma(1-\alpha)\,(t/\tau_m)^{\alpha}; \tag{28}$$

$$\alpha = 0, \quad \psi(t) \sim \frac{1}{\ln(\tau_M/\tau_m)} \left(C + \ln \frac{t}{\tau_m}\right), \tag{29}$$

where C is Euler's constant;

$$\alpha > 0, \quad \psi(t) \sim (\tau_m/\tau_M)^{\alpha}\,(t/\tau_m)^{\alpha}. \tag{30}$$

These are reminiscent of various transient rheologies observed on many materials. Once more, we note that $\Delta\psi$ is independent of the width of the spectrum if (18)–(20) are used, instead of (16). And again we note the influence of α on the rheology. For α negative, strain hardening is very rapid and the anelastic strain rapidly approaches an equilibrium value. For α positive, the larger density of slow retardation mechanisms obtains for times much longer than τ_m and anelastic strain continues to grow as a power-law. The intermediate value $\alpha = 0$ yields a logarithmic creep law.

(iii) *Long-time régime*, $\tau_m \ll \tau_M \ll t$

For such long times, all links have relaxed to their equilibrium, bowed position. The normalized creep function is exponentially close to unity in all cases. This stage is reached when all dislocation segments have reached the same equilibrium radius of curvature. This radius may be smaller than $0.5 l_M$, however, for large enough applied stress. In that case, an equilibrium configuration is never reached because the longer links begin to multiply and this gives rise to unbounded plastic strain. We shall return to this point later.

(*d*) *Attenuation properties*

In the frequency domain, the anelastic properties described above give rise to an absorption band with fairly simple properties. The basic concepts are found in Liu *et al.* (1976), and have been recently reviewed by Kanamori & Anderson (1977) and Minster (1980). Let V_u be the unrelaxed high-frequency wave velocity; the complex wavenumber is then given by

$$k^2(\omega) = \frac{\omega^2}{V_u^2}\left[1+\frac{\alpha\Delta}{\tau_M^\alpha-\tau_m^\alpha}\int_{\tau_m}^{\tau_M}\frac{d\tau}{\tau^{1-\alpha}(1+i\omega\tau)}\right], \tag{31}$$

which may be represented in terms of hypergeometric functions. As shown by O'Connell & Budiansky (1978), an unequivocal and convenient definition of the quality factor is

$$Q(\omega) = -\mathrm{Re}\,[k^2(\omega)]/\mathrm{Im}\,[k^2(\omega)]. \tag{32}$$

Although no simple analytical form can be derived for $Q(\omega)$, asymptotic expressions can be obtained fairly easily in the various régimes already mentioned. In the limit of a very narrow spectrum, the absorption band reduces to the classical Debye peak. For a broad spectrum, we consider three frequency bands.

(i) *Long periods*, $\omega\tau_m \ll \omega\tau_M \ll 1$

$$\alpha < 0, \quad Q(\omega) \sim -\frac{1+\alpha}{\alpha}\frac{1+\Delta}{\Delta}\left(\frac{\tau_M}{\tau_m}\right)^\alpha(\omega\tau_M)^{-1}; \tag{33}$$

$$\alpha = 0, \quad Q(\omega) \sim \left[\frac{1+\Delta}{\Delta}\ln\frac{\tau_M}{\tau_m}-1\right](\omega\tau_M)^{-1}; \tag{34}$$

$$\alpha > 0, \quad Q(\omega) \sim \frac{1+\alpha}{\alpha}\frac{1+\Delta}{\Delta}(\omega\tau_M)^{-1}. \tag{35}$$

$Q(\omega)$ is found to increase linearly with period, the classical behaviour of the long period side of an absorption band. For monochromatic waves at such periods, all dislocation links bow out to equilibrium and the medium exhibits relaxed elastic behaviour, with phase velocity

$$V_r \sim V_u/(1+\Delta)^{\frac{1}{2}}. \tag{36}$$

(ii) *Absorption band*, $\omega\tau_m \ll 1 \ll \omega\tau_M$

Asymptotic approximations are more laborious to derive in this case. We find:

$$\alpha < 0, \quad Q(\omega) \sim \cot\tfrac{1}{2}\alpha\pi - \frac{1+\Delta}{\Delta}\frac{\cos\frac{1}{2}\alpha\pi}{\frac{1}{2}\alpha\pi}(\omega\tau_m)^\alpha; \tag{37}$$

$$\alpha = 0, \quad Q(\omega) \sim \frac{1+\Delta}{\Delta}\frac{2}{\pi}\ln\frac{\tau_M}{\tau_m}-\frac{2}{\pi}\ln\omega\tau_M; \tag{38}$$

$$\alpha > 0, \quad Q(\omega) \sim \cot\tfrac{1}{2}\alpha\pi + \frac{1}{\Delta}\frac{\cos\frac{1}{2}\alpha\pi}{\frac{1}{2}\alpha\pi}(\omega\tau_M)^\alpha. \tag{39}$$

Depending on the sign of α, $Q(\omega)$ decreases or increases as ω^α. With $\alpha = 0$ Q is quasi-independent of frequency; this assumption is often used in seismology (see, for example, Liu *et al.* 1976; Anderson *et al.* 1976; Minster 1978*a*, *b*). A mild frequency dependence such as predicted by (39) has also been suggested by various authors (for example, Jeffreys 1970; Jeffreys & Crampin 1970; Macdonald 1961, 1963; Anderson & Minster 1980*a*, *b*; Strick 1970).

PHILOSOPHICAL TRANSACTIONS OF THE ROYAL SOCIETY A MATHEMATICAL, PHYSICAL & ENGINEERING SCIENCES

It is interesting to note that there is little generality to be gained by letting α take values outside the range $[-1, 1]$. A power-law dependence of $Q(\omega)$ on ω still holds, but $Q(\omega)$ cannot vary faster than ω or ω^{-1} within the framework of linear models such as the present one. Thus, a sharp drop of the relaxation spectrum is difficult to distinguish from a simple cut-off, insofar as the absorption band is concerned. The physical dispersion is obtained from the definition

$$k(\omega) = \omega/V_{\mathrm{p}}(\omega) - \mathrm{i}\gamma(\omega), \tag{40}$$

where $V_{\mathrm{p}}(\omega)$ is the phase velocity and $\gamma(\omega)$ the attenuation coefficient. Asymptotic results are conveniently derived only if $Q(\omega) \gg 1$, i.e. in the small-loss approximation. We have then

$$\alpha < 0, \quad V_{\mathrm{p}}(\omega) \sim V_{\mathrm{u}}[1 - \tfrac{1}{2}\Delta + \tfrac{1}{2}\cot \tfrac{1}{2}\alpha\pi Q^{-1}(\omega)]; \tag{41}$$

$$\alpha = 0, \quad V_{\mathrm{p}}(\omega) \sim V_{\mathrm{u}}[1 + (\pi \ln \omega\tau_{\mathrm{M}})^{-1}\, Q^{-1}(\omega)]; \tag{42}$$

$$\alpha > 0, \quad V_{\mathrm{p}}(\omega) \sim V_{\mathrm{u}}[1 - \tfrac{1}{2}\cot \tfrac{1}{2}\alpha\pi Q^{-1}(\omega)]. \tag{43}$$

Thus, for $\alpha \neq 0$, the phase velocity varies as a power of frequency, whereas $\alpha = 0$ yields the classical logarithmic dispersion.

(iii) *High frequencies*, $1 \ll \omega\tau_{\mathrm{m}} \ll \omega\tau_{\mathrm{M}}$

At high frequencies, none of the dislocation links reach their relaxed equilibrium configuration. Little anelastic strain takes place, and we have the following limiting behaviour:

$$\alpha < 0, \quad Q(\omega) \sim -\frac{1-\alpha}{\alpha\Delta}\,\omega\tau_{\mathrm{m}}; \tag{44}$$

$$\alpha = 0, \quad Q(\omega) \sim \frac{\ln(\tau_{\mathrm{M}}/\tau_{\mathrm{m}})}{\Delta}\,\omega\tau_{\mathrm{m}}; \tag{45}$$

$$\alpha > 0, \quad Q(\omega) \sim \frac{1-\alpha}{\alpha\Delta}\left(\frac{\tau_{\mathrm{M}}}{\tau_{\mathrm{m}}}\right)^{\alpha}\omega\tau_{\mathrm{m}}. \tag{46}$$

Once again, comparison with (17)–(20) shows that these limits are independent of the distribution of lengths when such a distribution controls the absorption band. This is consistent with our discussion of $\psi(t)$ for short times. On the other hand, the width of the band enters (45) and (46) explicitly when one considers a distribution of activation energies instead. The linear increase of Q with frequency is characteristic of the high-frequency side of an absorption band; $V_{\mathrm{p}}(\omega)$ asymptotically approaches V_{u} in that limit.

These properties are summarized in figure 2 which depicts three absorption bands with $\alpha = -0.25$, 0, and 0.25 respectively, as well as the associated dispersive characteristics of the medium.

The so-called high-temperature background internal friction in crystalline solids possesses the general characteristics derived above for intermediate and high frequencies (see, for example, Minster 1980). There is therefore a suggestion that laboratory frequencies are on the high-frequency–low-temperature side of an absorption band of the type discussed here. A similar relation appears to hold in the upper mantle at seismic frequencies (Anderson & Minster 1980*b*). Since an investigation of attenuation as a function of temperature depends critically on the activation energy, we defer discussion of these aspects until a specific physical model is considered.

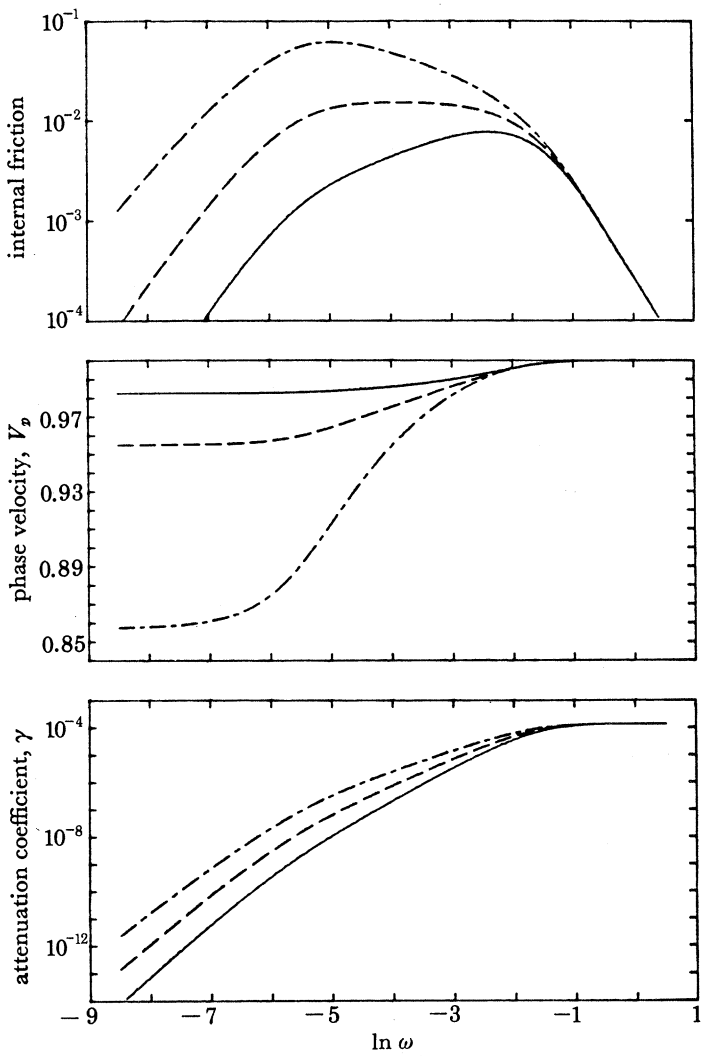

FIGURE 2. Three examples of absorption band and associated dispersion characteristics, for $\alpha = 0.25$, 0, and 0.25 respectively. $\tau_m = 1$ s, $\tau_M = 10^4$ s. Relaxation spectra have been adjusted to yield identical high-frequency behaviour.

3. STEADY-STATE RHEOLOGY

(a) *An idealized microstructural model*

For a given applied (tectonic) stress σ_t the equilibrium radius of curvature of the dislocation lines is obtained by solving (6) in the static limit

$$R_c = \mu b/2\sigma_t. \tag{47}$$

Links with lengths $l > l_c = 2R_c$ bow beyond a semi-circle and thereafter multiply, either through a Frank–Read mechanism, if glide only is permitted, or a Bardeen–Herring mechanism for glide plus climb. A crude estimate of the time required for multiplication is obtained by considering the midpoint of the link, and assuming that the link is a circular arc at all times during bowing out; then

$$t_\mu(l) = \int_0^{\frac{1}{2}l} V^{-1}(x)\, \mathrm{d}x, \tag{48}$$

where $V(x)$ is obtained by solving (6) for this geometry. The solution takes the form

$$t_\mu(l) = (l_c/2V_D)\, f(l/l_c), \tag{49}$$

where

$$f(x) = \tfrac{1}{2}x + \ln\left[\frac{2(x-1)}{x}\right]^{\frac{1}{2}} + \frac{1}{(x^2-1)^{\frac{1}{2}}} \arctan\left(\frac{x+1}{x-1}\right)^{\frac{1}{2}}. \tag{50}$$

Figure 3 is a graphical comparison of the relaxation time (9) and the multiplication time (49) under the same applied stress $\sigma = \sigma_s = \sigma_t$. It illustrates the region of validity of the anelastic theory developed in the previous section. For sufficiently large stress, l_c is shorter than some or all of the mobile links. These links multiply on a time scale $t_\mu(l)$ and we have non-recoverable plastic strain. The function $f(x)$ has a minimum for $x = 1.66$; thus links with $l = 1.66 l_c$ are the first to multiply. It is reasonable to expect that they will dominate the distribution of lengths in the long run since they are associated with the most efficient yielding process.

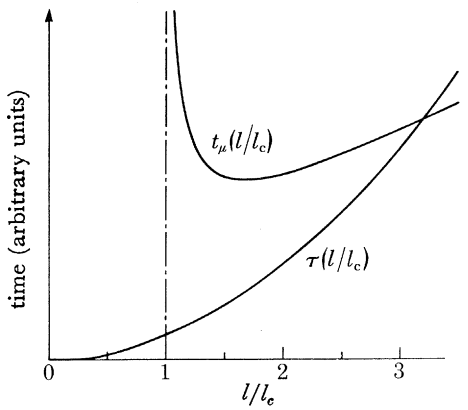

FIGURE 3. Comparison of relaxation time τ and multiplication time t_μ as function of dislocation length normalized by critical length.

According to this argument, we expect

$$l \approx 1.66\mu b/\sigma_t \approx \rho_m^{-\frac{1}{2}}. \tag{51}$$

The remarkable agreement with the observations of Durham *et al.* (1977) is undoubtedly fortuitous, but nevertheless gives some credence to this simple argument. It is noteworthy that this only differs slightly from the results of Takeuchi & Argon (1976*b*), which involve much more sophisticated modelling techniques.

Observations of subgrain dimensions in olivine compiled by Durham *et al.* (1977) are well fitted by a relation of the form

$$\bar{L} \approx K_s \mu b/\sigma_t, \tag{52}$$

with $15 \lesssim K_s \lesssim 50$. When combined with (51) and (3), this yields a constant K_m in the range 9–30. Under mantle conditions we may speculate that the material has been annealed over a very long period of time, so that intragrain dislocation density may be somewhat lower than in laboratory samples, and the degree of organization higher. These factors conspire to decrease the estimate of K_m, so that $K_m \approx 10$ may be an appropriate value, especially in view of the uncertainties involved. Thus emerges a microstructural model involving subgrains of dimension $\bar{L} \approx 20 l_c$, containing rather few mobile dislocations of mean length $l \approx 2l_c$. All lengths scale inversely with the long-term tectonic stress σ_t. If most dislocations are to be found in

cell walls so that ρ_w in (4) is indeed over an order of magnitude greater than ρ_m, then we must take the constant K in equation (5) to be greater than 30. We now explore the consequences of this highly idealized and simplified microstructure for various creep mechanisms.

(*b*) *Creep mechanisms*

A convenient method of comparison of rheological mechanisms is through their characteristic times. For steady-state creep we consider the Maxwell time

$$\hat{\tau} = \sigma_t/\mu\dot{\epsilon}, \tag{53}$$

where $\dot{\epsilon}$ is the strain rate. Reviews of possible creep mechanisms are provided by Weertmann (1970), Stocker & Ashby (1973) and Poirier (1976). For our purposes we shall compare three basic mechanisms: diffusional creep; dislocation creep controlled by intragrain recovery; and dislocation creep controlled by cell-wall recovery.

For diffusional creep we use the Nabarro–Herring creep equation in the form

$$\dot{\epsilon}_{\text{N.H.}} = C_{\text{N.H.}} \frac{D_s}{L^2} \frac{\sigma_t \Omega}{kT}, \tag{54}$$

so that

$$\hat{\tau}_{\text{N.H.}} = C_{\text{N.H.}} \left(\frac{\mu}{\sigma_t}\right)^2 \frac{kTb^2 \exp(E_s^*/RT)}{\mu D_{0s} \Omega}. \tag{55}$$

Here we have assumed the cell walls to be efficient sources and sinks of vacancies. D_{0s} and E_s^* are the pre-exponential diffusivity and activation energy for self-diffusion, and Ω is the atomic volume. $C_{\text{N.H.}}$ is a constant of order 20 (Stocker & Ashby 1973). This equation is easily generalized to include Coble creep.

For dislocation creep models we invoke the simple form of Orowan's equation discussed by Poirier (1976). At steady state, the hardening rate is exactly balanced by the recovery rate and the strain rate is expressed by

$$\dot{\epsilon} = \rho_m b(\Lambda/d) V. \tag{56}$$

Here, Λ is the mean free path of the dislocation; d is the distance covered at the rate-controlling speed V. Most models assume that $V = V_c$, the climb velocity, and that d is the distance covered by climb.

Takeuchi & Argon (1976*b*) have proposed a model where glide and climb are equally difficult, owing to the drag of a Cottrell atmosphere by edge segments. In that case the mean free path Λ is about equal to the critical length l and so is d. An upper bound to the creep rate, and thus a lower bound to the Maxwell time is obtained by taking $V = V_c$, and we may use (see, for example, Hirth & Lothe 1968)

$$V_c = 2\pi \frac{\sigma_t \Omega_v}{kT} \frac{D_{0s} \exp(-E_s^*/RT)}{\lambda_v}. \tag{57}$$

Here, Ω_v is the volume of a vacancy, and λ_v is a scale length associated with vacancy diffusion, of the form

$$\lambda_v \approx b \ln(r_2/r_1), \tag{58}$$

where r_1 and r_2 are inner and outer cut-off radii (see, for example, Hirth & Lothe 1968; Takeuchi & Argon 1976*b*; Poirier 1976). Typical values of the ratio r_2/r_1 for intragrain processes are of the order of 10^4, and the Maxwell time is found to be

$$\hat{\tau}_{\text{i.g.}} = C_{\text{i.g.}} \left(\frac{\mu}{\sigma_t}\right)^2 \frac{kTb^2 \exp(E_s^*/RT)}{\mu D_{0s} \Omega_v}, \tag{59}$$

which is of the same form as (55), but where the constant $C_{\text{i.g.}}$ is now of order unity. This mechanism is thus more efficient than the generalized Nabarro–Herring diffusion. The estimate (59) may be decreased further by $d/\Lambda \approx l/\Lambda$ if glide is somewhat easier than climb, and the mean free path of intracell dislocations is longer than l. But in that case we rapidly reach the point where many, if not most, dislocations actually collide with cell walls. Then a more appropriate model is one where recovery in subgrain boundaries plays a specific role. Such models have been reviewed by Weertman (1975) and by Poirier (1976), and a brief discussion is given by Minster & Anderson (1980). For Weertman's (1975) model with dislocation pile-ups, the Maxwell time $\hat{\tau}_{\text{p.u.}}$ is given by (59), where the proportionality constant is replaced by

$$C_{\text{p.u.}} = 1/0.006K_{\text{s}}^3. \tag{60}$$

Alternative models have been proposed which yield a stronger stress dependence of the creep rate. However, as noted by Weertman (1975) and Poirier (1976), they usually stem from *ad hoc* modifications of the σ^3 creep law which arise naturally under minimal assumptions. A model which involves explicitly the microstructural constant K is that of Gittus (1976*a*). The following is a simplified treatment of it, adapted for our purposes.

The mean free path of mobile dislocations is bounded from above by the subgrain size $\bar{L}$. In the limiting case where recovery takes place exclusively by climb in cell walls, we actually take $\Lambda = \bar{L}$. The mean separation between dislocations in cell walls is $r_{\text{w}} = \bar{L}/K^2$, and Gittus (1976*a*) gives the following expression for the steady-state creep rate:

$$\dot{\epsilon} = -\frac{\mathrm{d}r_{\text{w}}}{\mathrm{d}t}\Big/\frac{\mathrm{d}r_{\text{w}}}{\mathrm{d}\epsilon} = -V_{\text{c}}\Big/\frac{\mathrm{d}r_{\text{w}}}{\mathrm{d}\epsilon}.$$

This is equivalent to (56) if one notes that, for each length $\bar{L}$ of dislocation entering the cell walls after sweeping the cell cross-section, annihilation required to keep a constant density in the wall takes place by climb over a distance

$$d = \delta r_{\text{w}} \approx r_{\text{w}}^2/\bar{L} \approx \bar{L}/K^4. \tag{61}$$

In addition, climb in the cell walls may take place under conditions of jog under-saturation in vacancies (see, for example, Friedel 1964; Hirth & Lothe 1968); in that case, (58) must be replaced by (see, for example, Poirier 1976)

$$\lambda_{\text{v}} \approx 2\pi b c_j^{-1} = 2\pi b \exp\left(E_{\text{j}}/RT\right), \tag{62}$$

where c_{j} is the jog concentration along the dislocation line, and E_{j} is the jog formation energy. The Maxwell time is found to be

$$\hat{\tau}_{\text{c.w.}} = C_{\text{c.w.}} \left(\frac{\mu}{\sigma_{\text{t}}}\right)^2 \frac{kTb^2 \exp\left[(E_{\text{s}}^* + E_{\text{j}})/RT\right]}{\mu D_{0\text{s}} \Omega_{\text{v}}}, \tag{63}$$

where $C_{\text{c.w.}} \approx 3/K^4$. Cell-wall recovery is therefore a more efficient mechanism, and is a high-temperature mechanism since it possesses a higher effective activation energy.

In the cell-wall model of Gittus (1976*a*), the force causing climb is associated with the self-stress of the boundary network. Climb takes place so as to shorten the total dislocation length of the boundary and thus reduce the energy of the boundary. In this case, σ_{t} must be replaced in (57) by $\mu b/2r_{\text{w}}$. This mechanism is the more efficient one when

$$b/2r_{\text{w}} > \sigma_{\text{t}}/\mu. \tag{64}$$

This constraint is satisfied for $K^2 > 2K_s$. In that case, the estimate (63) for the Maxwell time remains valid, with a new value of the constant $C_{c.w.}$:

$$C_{c.w.} \approx 2K_s^3/K^6K_m^2. \tag{65}$$

The expression (57) for the climb velocity must be modified somewhat when the contribution of core diffusion is taken into account and when the wall dislocations are straight, with few geometrical jogs. In that case, the appropriate expression is (see, for example, Hirth & Lothe 1968, p. 528)

$$V_c = 4\pi \frac{\sigma_t \Omega_v}{kT} \frac{D_{0s} \exp\left[-(E_s^* + E_j - \frac{1}{2}\Delta E^*)/RT\right]}{b \ln(\bar{z}/b)}. \tag{66}$$

Here, ΔE^* is the difference between the activation energies for bulk diffusion and core diffusion, and $\bar{z}$ is the mean free path of vacancies along the dislocation line

$$\bar{z} \approx b\sqrt{2} \exp(\Delta E^*/2RT). \tag{67}$$

Expression (66) holds when jog spacing is larger than $\bar{z}$, that is when $E_j > \frac{1}{2}\Delta E^*$; in other words, it assumes undersaturation. It is easy to see that use of (66) yields again a Maxwell time of the form (63), although the activation energy is somewhat smaller. The constant $C_{c.w.}$ is not very different from (65):

$$C_{c.w.} \approx (2\pi)^{-1} \ln(\bar{z}/b)\, K_s^3/K^6K_m^2. \tag{68}$$

All the mechanisms considered so far (equations (55), (59) and (63)) lead to Maxwell times proportional to σ_t^{-2}; in other words, the creep rate, $\dot{\epsilon}$, varies as σ_t^3 in each case, and the main sources of variation among these models lie in the different constants and activation energies. A significantly different behaviour obtains when the Gittus cell-wall model is adopted, and climb is controlled by double jog nucleation. Indeed, in this model, the dislocation segments in the cell-wall networks have a length r_w which may be shorter than thermal jog separation. In that case the climb velocity (66) must be multiplied by $r_w c_j/b$ (Hirth & Lothe 1968, p. 528), and σ_t^2 dependence of the creep rate results (Minster & Anderson 1980). Note that this implies a high activation energy, and that $\hat{\tau}$ is only proportional to σ_t^{-1}. One might therefore expect this mechanism to dominate at high temperatures and low stresses, but this in turn would imply high thermal jog densities and longer dislocation segments, which might lead to a contradiction. Thus the existence of a domain in (T, σ_t)-space where this mechanism dominates depends on whether the inequality $r_w < bc_j^{-1}$ can be satisfied without violating microstructural scaling laws. This can be written

$$K^2 > K_s(\mu/\sigma_t) \exp(-E_j/RT), \tag{69}$$

which places a lower bound on the stress and/or an upper bound on the temperature if the other parameters are known. In that case we have

$$\left.\begin{aligned} \hat{\tau}_{sq} &= \hat{\tau}_{c.w.}(K^2/K_s) \exp(E_j/RT), \\ C_{sq} &= (K^2/K_s)\, C_{c.w.}. \end{aligned}\right\} \tag{70}$$

For applications to the Earth, we must correct the Maxwell time expression given above for the effect of confining pressure. This correction term is unfortunately quite uncertain. We shall assume that, for practical purposes, the only effect is to increase the effective activation energy by PV^*, where P is the pressure and V^* is an activation volume. In the absence of a simple and reliable theory for V^* when core diffusion takes place, it seems unjustified to attempt a more sophisticated treatment.

4. Applications and discussion

In view of the models presented above, attenuation and creep properties may be closely connected via the dislocation microstructure. We shall use the hypothesis that a single microstructural model explains both aspects of the rheology to place constraints on the model parameters.

(a) *Constraints on creep models*

The most stringent and useful constraints we can place on the various creep models outlined above is that they should satisfy laboratory data on olivine. These data have been summarized by Kohlstedt & Goetze (1974), Durham *et al.* (1977) and Goetze (1978). The range of stresses for which experimental data are available is 10^2–5×10^4 bar, but the class of models considered is probably only applicable for stresses smaller than 2 kbar (Goetze 1978; Kohlstedt 1979). Furthermore, since we are interested in large regions of the mantle where the tectonic stress is probably only a few bars, we must assume that extrapolation of laboratory trends to low stresses is possible, by means of the scaling laws described earlier.

Based on the general aspect of the microstructure, and on some observations on dislocation glide, Durham *et al.* (1977), and Goetze (1978) suggest that Takeuchi's & Argon's (1976*b*) creep model (e.g. equation (59)) may be appropriate for laboratory-deformed olivine, in the approximate range 100–2000 bar. The comparison is qualitative, however, and no numerical comparison was given. We have already shown (Anderson & Minster 1980*b*), that a straightforward application of Gittus's (1976*a*) creep model could explain observations quantitatively. In this paper, we consider a more general class of models and compare them systematically against various observational constraints, starting with direct estimates of some physical parameters.

(i) *Self-diffusion*

When multi-species coupled diffusion takes place, self-diffusion is largely controlled by the bulk-diffusion of the slowest moving species (see, for example, Stocker & Ashby 1973). In silicates, this has long been thought to be oxygen (see, for example, Ashby & Verrall 1978; Sammis *et al.* 1977). A recent estimate of the diffusivity of oxygen in forsterite is (Reddy *et al.* 1980)

$$D(\mathrm{O}) = 3.5 \times 10^{-3} \exp(-89\,000/RT)\ \mathrm{cm^2/s}.$$

Recently, however, a lower diffusivity has been found for silicon (Jaoul *et al.* 1979; Poumellec *et al.* 1980):

$$D(\mathrm{Si}) = 1.5 \times 10^{-6} \exp(-90\,000/RT)\ \mathrm{cm^2/s}.$$

In this paper we shall consider either alternative to be possible and present results for both cases. In Mg_2SiO_4, the appropriate atomic volume Ω appearing in (55) is one-quarter the molecular volume (7.2 $\mathrm{cm^3/mol}$) if oxygen is the controlling species, and the total molecular volume (28.8 $\mathrm{cm^3/mol}$) if silicon is the controlling species (Stocker & Ashby 1973).

Undoubtedly a similar distinction should be made about the vacancy volume Ω_v in the dislocation creep models. Such differences are rather trivial, however, compared with uncertainties in the other parameters. We shall make the simple choice

$$\left.\begin{aligned} E_s^* &= 90\ \mathrm{kcal/mol}, \quad D_{0s} = \begin{cases} 3.5 \times 10^{-3}\ \mathrm{cm^2/s} & (\mathrm{O}), \\ 1.5 \times 10^{-6}\ \mathrm{cm^2/s} & (\mathrm{Si}), \end{cases} \\ \Omega_v &\approx b^3, \quad b \approx 7 \times 10^{-8}\ \mathrm{cm} \quad \text{(Stocker \& Ashby 1973).} \end{aligned}\right\} \tag{71}$$

(ii) *Creep activation energy*

The various models of dislocation creep at our disposal entail activation energies which result from combinations of poorly known quantities, such as jog formation energy, etc. On the other hand, the creep activation energy for olivine at high temperature has been estimated from laboratory observations. Recent interpretations of experimental data converge to a value of 125 ± 3 kcal/mol (Kohlstedt & Goetze 1974; Durham & Goetze 1977; Ashby & Verrall 1978; Goetze 1978).

Our approach is to assume that the creep activation energy is $E_c^* = 125$ kcal/mol and to consider the variation of unknown quantities subject to this constraint. Thus for cell-wall climb under applied stress (equation (63)) we have

$$E_s^* + E_j = 125 \text{ kcal/mol}; \quad E_j = 35 \text{ kcal/mol}. \tag{72}$$

For cell-wall climb under self-stress, and core diffusion (equation (65)) we have

$$E_j - \tfrac{1}{2}\Delta E^* = 35 \text{ kcal/mol}. \tag{73}$$

Here ΔE^* is the difference between the activation energy for bulk diffusion and that for core diffusion. For many metals, $\frac{1}{3}E_s^* \lesssim \Delta E^* \lesssim \frac{1}{2}E_s^*$ (see, for example, Hirth & Lothe 1968). On the other hand, we have argued (Anderson & Minster 1980*b*) that ΔE^* may be close to zero for olivine, since activation energies for hot-pressing experiments (Schwenn & Goetze 1978) and dislocation-loop mobility (Goetze & Kohlstedt 1973) do not yield activation energies much lower than E_s^* and E_c^*, respectively.

For our purposes, we shall consider the entire range $0 \leqslant \Delta E^* \leqslant \frac{1}{2}E_s^*$. For the σ^2 creep law (equation (70)), the constraint (73) must be rewritten as

$$2E_j - \tfrac{1}{2}\Delta E^* = 35 \text{ kcal/mol}. \tag{74}$$

Equations (73) and (74) lead to the following respective ranges for the jog formation energy E_j:

$$35 < E_j < 58 \text{ kcal/mol}; \tag{75}$$

$$17 < E_j < 29 \text{ kcal/mol}. \tag{76}$$

These ranges indicate much higher values than for metals (see, for example, Friedel 1964), an acceptable conclusion in view of the greater cell sizes, and the higher Peierls energies involved in silicates. These values may also be compared with the estimate of 26 kcal/mol for the kink energy suggested by Stocker & Ashby (1973); jog energies should indeed be greater than kink energies (Hirth & Lothe 1968). The ranges (75) and (76) involve much smaller values than the geometrical estimates of order $0.1\mu b^3$: 100–300 kcal/mol (Friedel 1964). Admittedly, there is great uncertainty about geometrical estimates (Hirth & Lothe 1968), even in the case of the simplest metallic crystal structures. In the absence of a suitable theory for silicates, we *hypothesize* that the discrepancy between E_c^* and E_s^* is an empirical measure of the jog formation energy, subject to the constraint equations (73) or (74) if core diffusion takes place.

(iii) *Microstructural constants*

The scaling constants K_s and K_m can be estimated directly from the observations of Durham *et al.* (1977). Again these estimates are subject to fairly large uncertainties, and there is no guarantee that they can be used for extrapolation to mantle conditions. We take $K_s = 15$ and

$K_m = 10$; these values lie in the lower range of observations, and we have already argued that they may be appropriate. The constant K will be treated as a model parameter in our discussion. Domains of validity of the various creep models can be summarized as follows:

For cell-wall climb under self-stress instead of applied stress (equation (64))

$$K^2 > 2K_s. \tag{77}$$

For the σ^2 creep law to be permissible (equation (69))

$$K^2 > K_s(\mu/\sigma_t) \exp(-E_j/RT). \tag{78}$$

An additional constraint must be placed on K for cell-wall recovery models with climb under jog undersaturation in vacancies. It places an upper bound on dislocation separation in the walls: $r_w/b = n_w < n_c$, where n_c is a critical number of lattice spacings of the order of $\exp(E_j/RT)$, which is large in the present applications. It is commonly assumed that saturation occurs if the separation is of the order of $10^4 b$, for example in subgrains (Friedel 1964). We shall assume, rather arbitrarily, that n_c is at least a factor of 10 smaller ($n_c < 1000$), although this concept is not very clear. If the transmission electron micrographs presented by Durham *et al.* (1977) are assumed to be typical, then n_w appears to be of the order of a few hundred for applied stresses of a few hundred bar. The constraint can be written

$$K^2 > K_s \left(\frac{\mu}{\sigma_t}\right) \frac{1}{n_c}. \tag{79}$$

If it fails to be satisfied, then saturation may take place and the climb velocity is of the form (57); jog formation is not a controlling process. On the other hand, as we mentioned earlier, for straight cell-wall dislocations, with few geometrical jogs, thermal jog pair nucleation is important and the saturation condition is simply (see, for example, Hirth & Lothe 1968)

$$E_j > \tfrac{1}{2}\Delta E^*. \tag{80}$$

This is always satisfied under constraint (73), and under constraint (74) it implies that $\Delta E^* < 70$ kcal/mol.

(iv) *Maxwell times*

As shown by Goetze (1978), creep data on olivine at stresses greater than about 2 kbar are well fitted by a Dorn creep law. Below 2 kbar a power-law creep appears to give a reasonable interpretation. Figure 4 shows the creep data of olivine collected from a variety of published sources by Kohlstedt & Goetze (1974), and supplemented with the creep observations of Durham & Goetze (1977) on olivine single crystals with odd orientations (their figure 4). All data have been reduced to a common temperature of 1673 K by using an activation energy of $E_c^* = 125$ kcal/mol.

The observations of creep rate below 2 kbar can support either an $\dot{\epsilon} \propto \sigma^3$ or an $\dot{\epsilon} \propto \sigma^2$ interpretation, and the scatter does not allow us to restrict the number of acceptable models on that basis alone. The bulk of the data, and detailed observations on individual samples by Durham & Goetze tend to support the higher exponent, but the lower stress observations seem to indicate a less sensitive stress dependence of the creep rate. As indicated on the figure, this can result in variations of several orders of magnitude in the extrapolated creep rate at 10 bar, in addition to the intrinsic scatter.

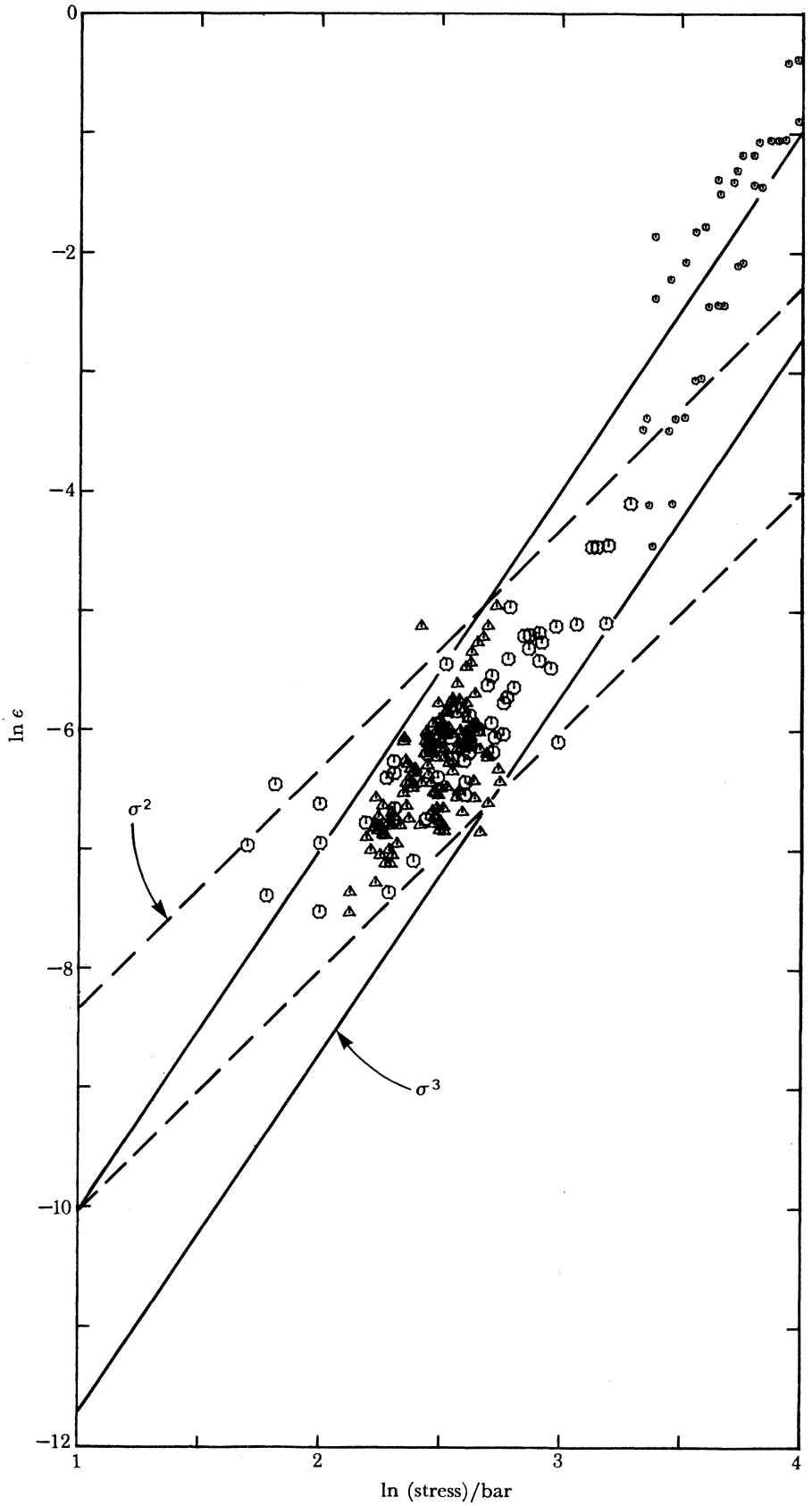

FIGURE 4. Steady-state creep rate observations in olivine compiled by Kohlstedt & Goetze (1977) (circles) supplemented by observations of Durham & Goetze (1974) (triangles), as a function of applied stress. Data for stresses greater than 2000 bar are shown by smaller symbols.

PHILOSOPHICAL TRANSACTIONS OF THE ROYAL SOCIETY A MATHEMATICAL, PHYSICAL & ENGINEERING SCIENCES

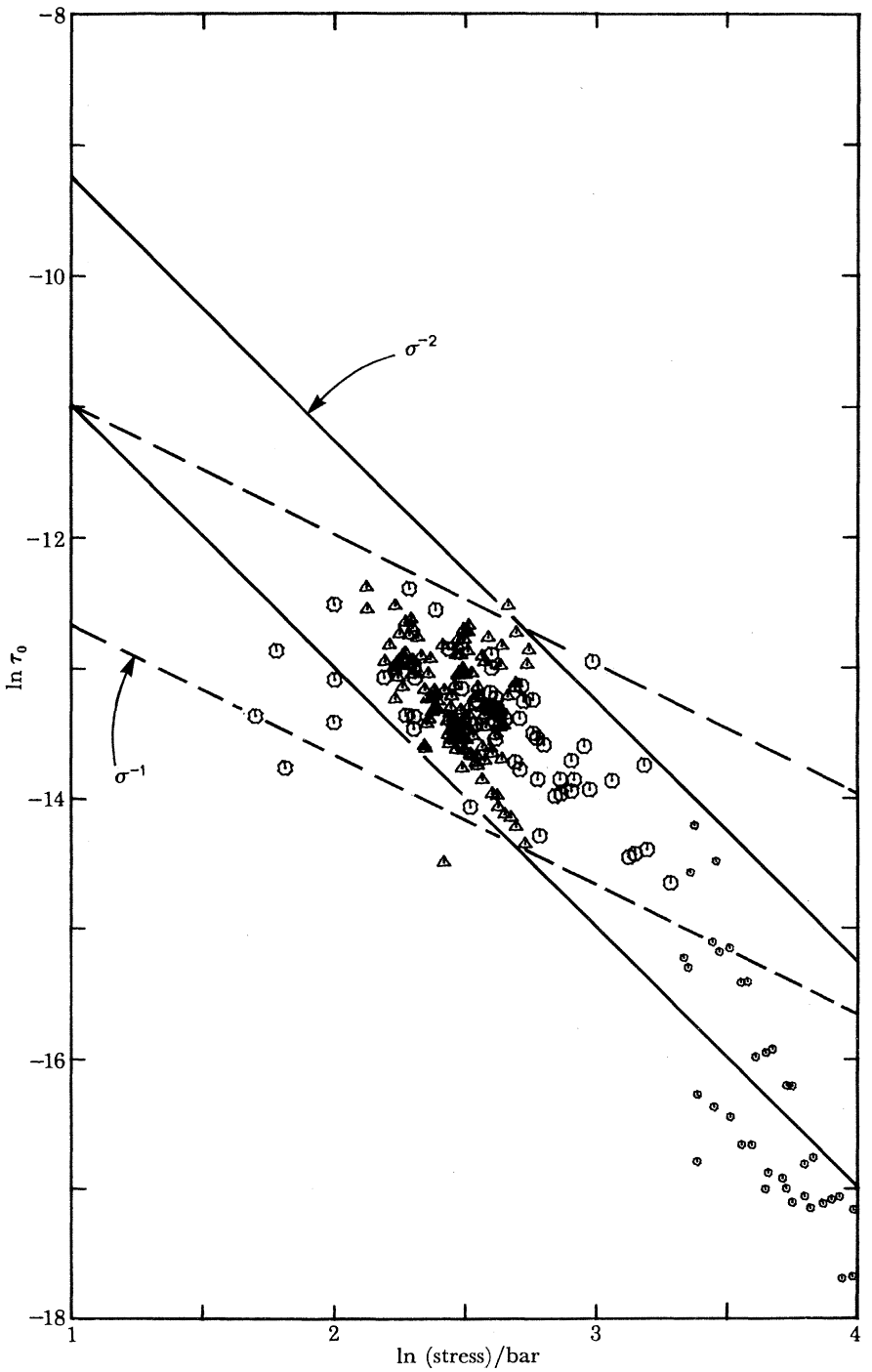

FIGURE 5. Data as for figure 4, converted to Maxwell times, assuming a rigidity $\mu = 650$ kbar.

PHILOSOPHICAL TRANSACTIONS OF THE ROYAL SOCIETY A MATHEMATICAL, PHYSICAL & ENGINEERING SCIENCES

Each data point in figure 4 was converted into a pre-exponential Maxwell time $\hat{\tau}_0$, by using a rigidity of 650 kbar. The resulting stress dependence is shown on figure 5, together with the σ^{-2} and σ^{-1} extrapolations to low stress, corresponding to the alternate interpretations of figure 4. Approximate ranges for $\hat{\tau}_0$ at 10 bar are:

$$\left.\begin{aligned} &\text{for } \sigma^3 \text{ creep laws,} && \hat{\tau}_0(10\text{ bar}) \approx 10^{-11}\text{–}10^{10}\text{ s;} \\ &\text{for } \sigma^2 \text{ creep,} && \hat{\tau}_0(10\text{ bar}) \approx 2\times10^{-13}\text{–}10^{-11}\text{ s.} \end{aligned}\right\} \tag{81}$$

We use these ranges as observational constraints to compare the various models discussed in the previous section.

(*b*) *Comparison of creep models*

A convenient procedure to compare the various models is to compute the predicted Maxwell time pre-exponential factor $\hat{\tau}_0(1673, 10)$ at a fixed temperature (1673 K) and stress (10 bar).

(i) *Diffusional creep* (*equation* (55))

According to the preceding discussion, we do not have any free parameters left in this model. If oxygen diffusion is rate controlling, we find $\hat{\tau}_0(1673, 10) \approx 3.7\times10^{-3}$ s, and, if silicon diffusion is rate controlling, we find $\hat{\tau}_0 \approx 2.1$ s. These values are many orders of magnitudes too large and we can eliminate this possibility. In addition, the predicted activation energy is 90 kcal/mol, which is much smaller than the observed value.

(ii) *Intracell recovery creep* (*equation* (59))

In that case, we find

$$\hat{\tau}_0 \approx 6.2\times10^{-6}\text{ s} \quad \text{for oxygen diffusion,}$$

$$\hat{\tau}_0 \approx 1.4\times10^{-2}\text{ s} \quad \text{for silicon diffusion.}$$

These estimates are still much too large to satisfy laboratory observations, and the predicted activation energy of 90 kcal/mol is too small. We may therefore eliminate this model as well.

(iii) *Pile-up model* (*equation* (60))

If oxygen controls self-diffusion, constraint (81) requires $130 \lesssim K_s \lesssim 470$. This range becomes $1700 \lesssim K_s \lesssim 6200$ if silicon is rate controlling. These values are much larger than the observed range. Furthermore, the predicted activation energy is 90 kcal/mol. We must therefore turn to a more flexible model.

(iv) *Cell-wall recovery under applied stress* (*equation* (63))

We now have the parameters K and E_j at our disposal. As pointed out earlier, a jog formation energy of 35 kcal/mol would reconcile the activation energy with the observed value. If oxygen is the controlling species for bulk diffusion, then, at 10 bar and 1673 K, $\hat{\tau}_0 \approx 1.84\times10^{-5}/K^4$ s; when combined with the constraints (81), this results in $14 \lesssim K \lesssim 37$. If silicon is the controlling species, we get $96 \lesssim K \lesssim 256$. Thus, if silicon controls self-diffusion, the data require a very pronounced concentration of the dislocation population in the cell walls, ρ_w being two to three orders of magnitudes greater than ρ_m. If oxygen controls self-diffusion, then ρ_w is only required to be one order of magnitude, or less, greater than ρ_m.

In either case, however, K is too large to satisfy constraint (77). In other words, the model is self-invalidating if the concept of cell-wall climb under self-stress can be applied.

(v) *Cell-wall recovery under self-stress* (*equations* (64)–(65))

Testing of this modelling hypothesis proceeds in the same fashion as above. We must postulate a jog formation energy of $E_j = 35$ kcal/mol to reconcile the activation energies. If oxygen controls self-diffusion, then at 10 bar and 1673 K, $\hat{\tau}_0 \approx 4.14 \times 10^{-4}/K^6$ s; the observational constraints (81) yield in that case $9 \lesssim K \lesssim 19$. If silicon is the controlling species, we get $35 \lesssim K \lesssim 68$.

Thus if oxygen is the controlling species, the data imply a rather low range for K. In fact, it would be legitimate to argue that the microstructure would be so poorly defined that an intracell recovery model should really be considered. We have already seen, however, that this model does not appear to be successful.

The hypothesis that silicon-controlled self-diffusion limits the recovery rate by climb in cell walls under self-stress is a more attractive one. The density of cell-wall dislocations ρ_w is predicted to be one order of magnitude, or more, greater than the density of intracell, mobile dislocations ρ_m, in accordance with the premises of this model. This model cannot be rejected by our testing procedure.

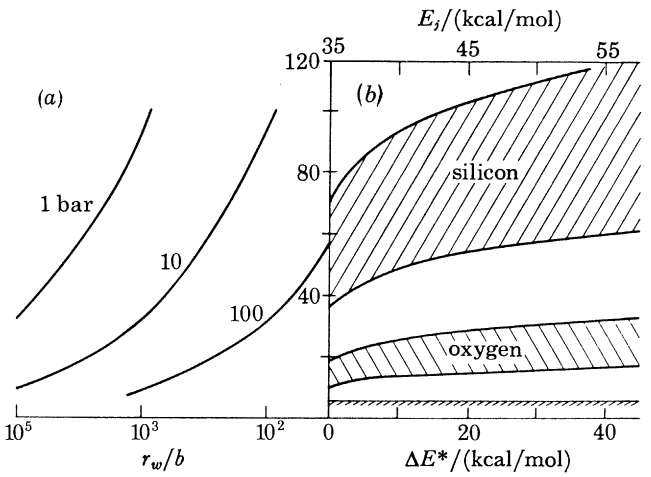

FIGURE 6. (*a*) Structural parameter K as a function of difference between bulk diffusion and core diffusion, for cell-wall recovery model controlled by double jog nucleation. Also indicated is the jog formation energy, which yields a creep activation energy of 125 kcal/mol (equation (73)). (*b*) The dislocation separation in the cell walls, for various values of the applied stress. Shaded areas indicate range of K-values which bracket laboratory data shown on figure 5. Forbidden area for this model (equation (77)) is also indicated.

(vi) *Cell-wall recovery controlled by double jog nucleation and core diffusion* (*equations* (66)–(68))

This model is a generalization of the previous one. We have now the extra parameter ΔE^* at our disposal. The variation of K implied by the constraints (81), as ΔE^* varies from 0 to $\frac{1}{2}E_s^*$, is shown in figure 6. The results are shown under the alternative hypotheses that oxygen or silicon controls self-diffusion.

Once more, the results for oxygen tend to conflict with the premises of the microstructural model, whereas the results for silicon yield a self-consistent picture, except possibly at very low stresses of the order of 1 bar, for which dislocation spacing in cell walls is large even with sizeable values of K. This model is thus an acceptable alternative to the previous one, especially if

further experiments should indicate a low activation energy for core diffusion, and a concomitantly high jog formation energy.

The data available now, although rather limited and indirect, tend to point to low values of ΔE^* (Anderson & Minster 1980*b*); in that case the approximate range is $40 \lesssim K \lesssim 80$, pointing to a sharply defined microstructure.

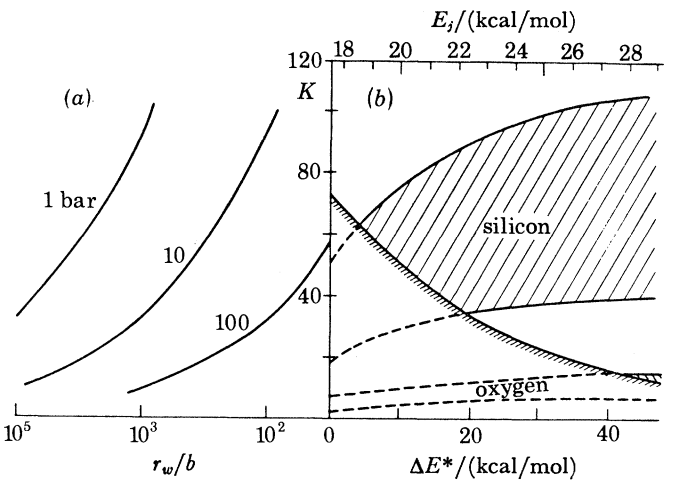

FIGURE 7. As for figure 6, for σ^2 creep law. Jog formation energy calculated by (74). Forbidden area corresponds to (78).

(vii) σ_t^2 *creep law* (*equation* (70))

This law applies to a cell-wall model where cell-wall dislocation segments are shorter than the thermal jog separation. This leads to the constraint (78), and interpretation of the observations in terms of this rheology leads to the second set of bounds on $\hat{\tau}_0(1673, 10)$ in (81). If oxygen diffusion controls the self-diffusion rate, then this model is unacceptable and must be rejected, as can be seen on figure 7; it does not satisfy (78) for admissible core diffusion activation energies. If silicon is the controlling species, then, once more, a range of satisfactory values of K is obtained. The model is generally associated with quite low values of E_j, however, and is also incompatible with our conjecture that ΔE^* is small. We must therefore consider it to be less satisfactory than the previous ones.

(*c*) *Creep in the mantle*

The systematic comparison of available models made above does not yield a unique acceptable model for low-stress, high-temperature creep. However, two general models satisfy all of our criteria self-consistently. Both involve cell-wall recovery under self-stress, both assume that silicon controls self-diffusion, and both can be accommodated by the same microstructure, with $40 \lesssim K \lesssim 70$; either model constitutes a generalization of the creep model originally developed by Gittus (1976*a*). Their only major difference is that core diffusion is ignored in one model, and accounted for in the other. Note that both models do not quite coincide for $\Delta E^* = 0$, owing to various approximations made in estimating the climb velocity (see, for example, Hirth & Lothe 1968).

To assess the applicability of our model to mantle rheology, we have calculated the Maxwell times for a range of applied stress from 1–1000 bar, as a function of temperature, and for

pre-exponential factors compatible with laboratory observations. For simplicity we have chosen $\hat{\tau}_0 \approx 7 \times 10^{-11}$ s at 10 bar, noting however that laboratory evidence can allow for values about five times larger or smaller. This in turn corresponds to $K \approx 50$, which means that the total length of dislocations in cell walls is 25 times greater than the total length of intracell dislocations.

The results are displayed in figure 8. Also shown is a box outlining a plausible range of mantle environments, for comparison only (temperatures from 1000–1800 °C; viscosity from 10^{19} to 10^{24} poise). Thus the model can easily accommodate geophysical observations quantitatively. This calculation ignores the effect of confining pressure, however, and this brings a new complication to the problem.

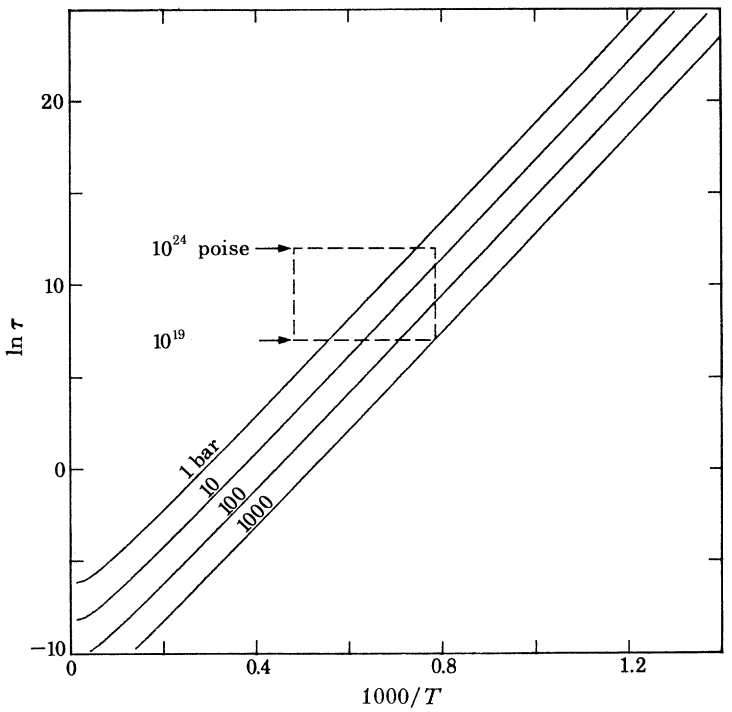

FIGURE 8. Temperature dependence of Maxwell time for several values of applied load, for a creep model which satisfies laboratory observations with a σ^3 interpretation.

In multispecies diffusion, the total activation volume for diffusion of the ith species is (see, for example, Stocker & Ashby 1973)

$$V_i^* = \frac{\alpha V_A + \beta V_B + \gamma V_C + \delta V_D + \dots}{\alpha + \beta + \gamma + \delta + \dots} + V_m^i, \tag{82}$$

where $\alpha, \beta, \dots$ are stoichiometric coefficients; $V_A, V_B, \dots$ are atomic volumes of individual species; and V_m^i is the activation volume for motion of the ith species, which we assume to be close to an atomic volume. For Mg_2SiO_4, this leads to 11 cm³/mol for oxygen, and about 4 cm³/mol for silicon. The preferred ranges of values of Sammis *et al.* (1977) for the mantle decrease from 11 to *ca.* 6 cm³/mol for the upper mantle, and from 6 to 3 cm³/mol for the lower mantle. They point out that this bounds the total variation of viscosity across the transition region (300–1000 km) to be less than two orders of magnitude. This argument was used

in reverse by Anderson & Minster (1980*a*), based on the modelling work of Peltier (1980), to argue for an effective activation volume between 4 and 9 cm^3/mol.

If we ignore for the moment the pressure dependence of the activation volume, the estimates for silicon and oxygen given above have an interesting and potentially important implication. Should silicon be the controlling species, then the pressure correction to the effective creep activation energy is about $0.1P$ kcal/mol, where P is in kilobars; this correction is about $0.27P$ kcal/mol if oxygen is the controlling species. If we now fix the microstructural model,

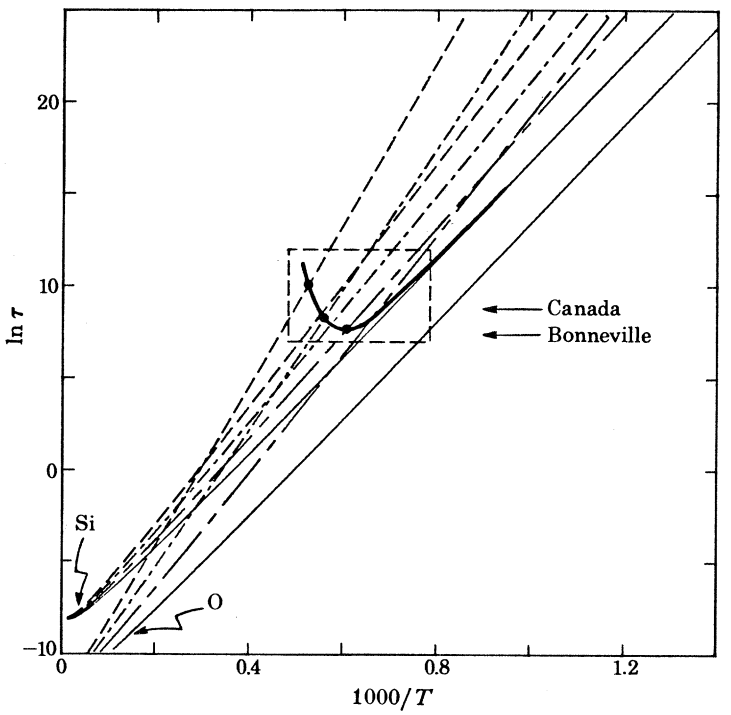

FIGURE 9. Effect of confining pressure on Maxwell times. At pressures greater than 200 kbar, oxygen diffusion becomes slower and controls self-diffusion. Simple thermal model of the mantle is shown, and compared with Crough's (1977) estimates for isostatic rebound. P/kbar: ——, 0; — — — —, 100; – – –, 200; – – –, 300.

the Maxwell time pre-exponential factors under both hypotheses are practically in the ratio of the diffusivities. At zero pressure this ratio is essentially independent of temperature because the activation energies are almost identical. According to our systematic evaluation of creep models, oxygen diffusion is then too rapid to satisfy the laboratory observations, and silicon diffusion appears to be rate controlling. The effect of pressure may reverse these roles, as shown in figure 9. We calculated Maxwell times for a fixed load of 10 bar ($\hat{\tau}_0 = 7 \times 10^{-11}$ for silicon diffusion), under the alternate hypotheses that silicon or oxygen are the controlling species, and for confining pressures up to 300 kbar. Because of the larger activation volume assumed for oxygen diffusion, we find that oxygen becomes the slower species at high pressure for a fixed temperature. As an indication of mantle conditions, we considered a geotherm with a linear temperature gradient of 0.3 °C/km, and a temperature of 1700 K at 400 km depth, and plotted the corresponding trajectory on figure 9. The switchover from silicon-controlled diffusion takes place at a pressure between 100 and 200 kbar (300 to 600 km depth).

Activation volumes are expected to decrease with increasing pressure based on an elastic

continuum model (see, for example, O'Connell 1977; Sammis *et al.* 1977). In applying (82), it is clear that the activation volume for silicon diffusion is controlled in turn by the much larger atomic volume of oxygen. As a result, it can be expected that both estimates of the activation volume might decrease at depth in about the same proportion. This will have two consequences: (i) the switch-over from silicon-controlled diffusion to oxygen-controlled diffusion will happen at greater pressure and thus greater depth; and (ii) the smaller activation volume in the lower mantle will tend to limit the variations of apparent viscosity with depth (Sammis *et la.* 1977).

These comparisons are very crude, and the results can vary considerably with model parameters. We have ignored chemical variations, changes in lattice structure with pressure, effects of water content on the activation energy, etc. Our microscopic models are probably not yet precise enough to support such sophistication. However, some general inferences can be made, which are robust with respect to the variations in interpretative models. For example, at mantle temperatures, very low effective viscosities (as low as 10^{15} poise) would be observed under loads of 1 kbar. Thus the model precludes the persistence of such loads for times longer than the corresponding Maxwell time (*ca.* 10^3 s). Loads of the order of 100 bar might explain the low apparent viscosities inferred by Nur & Mavko (1974) on the basis of post-seismic rebound data. On the other hand, persistent loads of the order of 10^3 bar can be sustained by a cold lithosphere over geological times (see, for example, Anderson & Minster 1980*a*; Minster & Anderson 1980). Reinterpretation of isostatic rebound data in terms of a phenomenological power-law flow compatible with our models was performed by Crough (1977). His analysis is a particularly striking illustration of the trade-offs between temperature, confining pressure, and applied load, of the kind shown in figures 8 and 9. His results, for an applied load of 10 bar, yield Maxwell times of 3.5×10^8 s for the Canadian shield and 1.7×10^7 s for Bonneville. As seen on figure 9, this is in good quantitative agreement with the predictions from the microscopic model.

(*d*) *Constraints on attenuation*

To discuss attenuation, we may recast (9) in a form comparable to the expressions for the Maxwell time by introducing the critical length l_c (see, for example, figure 3):

$$\tau = C_Q \left(\frac{\mu}{\sigma_t}\right)^2 \frac{kT \exp\left(E_Q^*/kT\right)}{\mu D_{0Q} \lambda}; \tag{83}$$

$$C_Q = \frac{2}{\pi^2}\left(\frac{l}{l_c}\right)^2; \tag{84}$$

where l_c is the critical length associated with the long-term background ('tectonic') stress σ_t. The most interesting implication of this formalism is, of course, that, to ensure consistency with the argument leading to (51), we must now postulate a very narrow distribution of lengths, clustered about the value $l = 1.66 l_c$. This has several important consequences.

The first and most straightforward is that the relaxation strength is given by (16), and, if the scaling law (51) holds, Δ is of the order of 10 % and is independent of stress.

The second consequence is that the absorption band itself depends strongly on the background tectonic stress. It shifts to high frequency with increasing stress and to low frequency with decreasing stress. Comparison of (83) with the Maxwell time yields, in fact,

$$\tau \sim \frac{C_Q}{C_{c.w.}} \frac{b}{\lambda} \frac{D_{0s}}{D_{0Q}} \exp\left[(E_Q^* - E_C^*)/RT\right] \hat{\tau}_{c.w.}. \tag{85}$$

Thus, given microscopic models for creep and attenuation – in particular, given the diffusivities and activation energies – we have a formal connection between steady-state creep, attenuation and tectonic stress, through the microstructure. This opens the possibility of formalizing the empirical correlations studied, for example, by Anderson (1966), Meissner & Vetter (1979) and Berckhemmer *et al.* (1979) within the framework of a physical model.

The third major consequence of requiring the microstructure to be compatible with the creep model is that a distribution of lengths is no longer available. Thus (12) cannot be at the source of a broad absorption band. To get a spread of pre-exponential factors, we must turn to a distribution either of D_{0Q} or of λ. The alternative, of course, is to rely on a distribution of activation energies to broaden the absorption band. In that case, the width and intensity of the band depends mainly on temperature, but its position along the frequency or temperature axis depends on the tectonic stress σ_t.

Numerous authors have considered diffusion-controlled dislocation damping as a possible mechanism for anelastic attenuation at low frequencies. A fairly recent treatment is that of Simpson & Sosin (1972). Some of the main alternatives are listed below.

(i) *Peierls barrier model of the Bordoni peak*

A Peierls barrier model of the Bordoni peak gives a relaxation time of the correct form. If we use the simplified theory of Hirth & Lothe (1968, p. 500), the activation energy is $2E_k$, where E_k is the kink formation energy, estimated to be *ca.* 26 kcal/mol by Stocker & Ashby (1973). The pre-exponential diffusivity is $D_{0Q} \approx \nu b^2$, where ν is an atomic frequency of the order of $10^{13}\,s^{-1}$, so that $D_{0Q} \approx 10^{-3}$–$10^{-2}\,cm^2/s$. The scale length λ is found to be $\lambda \approx C_Q l \times (\mu/\sigma_t)^2\,(\sigma_i/\mu)$, where σ_i denotes the internal stress. For intragrain processes, with few dislocations, σ_i is expected to be controlled mainly by the line tension (Gittus 1976*a*), and thus to be comparable to σ_t. λ is therefore of order $l\mu/\sigma_t$ and τ_0 is of the order of 10^{-15}–10^{-16} s, and is practically independent of σ_t. We have, therefore, a high-frequency, low-temperature mechanism, which does not operate in the seismic band and in the mantle. A more detailed review of the Bordoni peak is given by Nowick & Berry (1972).

(ii) *Glide controlled by kink diffusion*

Glide controlled by kink diffusion (Hirth & Lothe 1968, p. 497) might be appropriate in view of the high Peierls energy of olivine (see, for example, Gueguen 1979). For an initially straight segment of length l, bowing-out by kink pair generation and diffusion we have

$$\lambda \sim 2bl/[l + b \exp(E_k/RT)], \tag{86}$$

$$D_Q \sim \nu b^2 \exp(-E_k/RT), \tag{87}$$

Two circumstances may arise, depending on which term dominates the denominator of (86).

Let us assume that $E_k = 26$ kcal/mol (Stocker & Ashby 1973), and that $\sigma_t = 10$ bar. Then, for temperatures lower than the transition temperature $T_t = 1120$ K we have $\lambda \approx 2l \exp(-E_k/RT)$. The effective activation energy is then $E_Q^* \approx 2E_k \approx 52$ kcal/mol, and we have $\tau_0 \approx 10^{-12}$ s. Above T_t, we have $\lambda \approx 2b$, $E_Q^* \approx 26$ kcal/mol, and $\tau_0 \approx 10^{-7}$ s. In either case this yields an absorption band at much higher frequency than the seismic band. It must be recognized, however, that the kink formation energy is very uncertain, and that the transition temperature is very sensitive to both E_k and σ_t, as shown in table 1. Thus, for $\sigma_t = 10$ bar and $E_k = 35$ kcal/mol, we find $\tau_0 \approx 5 \times 10^{-12}$ s, $E_Q^* \approx 70$ kcal/mol, and the absorption band

approaches 1 Hz near 1500 K and longer periods at lower temperatures. This mechanism is therefore a potential candidate, particularly in regions where the stress is fairly high and the temperature fairly low, such as in the lithosphere.

TABLE 1. TRANSITION TEMPERATURE T_t/K

E_k / kcal/mol	σ_t/bar: 1	10	100
25	540	1080	1350
35	1250	1510	1885
45	1620	1940	2420

(iii) *Glide of jogged screw dislocations*

Yet another alternative is provided by the glide of jogged screw dislocations, where the jogs can only move by the production or absorption of point defects (Hirth & Lothe 1968, p. 535). In that case the diffusivity D_{0Q} is that for self-diffusion D_{0s}, which in turn is related to the diffusion of oxygen or silicon according to our discussion of creep. For small stresses we have $\lambda = 4\pi b/c_j$, where c_j is the jog concentration. Two cases arise: either the jogs are geometrical, and λ is of order b to within one or two orders of magnitude, $E_Q^* \approx E_s^* = 90$ kcal/mol; or the dislocation segments lie in Peierls valleys and we must consider thermal jogs (Gittus 1976*a*). In the latter case λ is $4\pi b$ and the activation energy is $E_Q^* \approx E_s^* + E_1 \geqslant 125$ kcal/mol in accordance with the creep model. In either case it is easy to verify that the retardation time is many orders of magnitude longer than the seismic periods. For example, under an applied stress of 10 bar, we get $\tau \approx 10^{13}$ s at 1600 K if silicon controls self-diffusion and thermal jogs are the dragging defects. On that basis, Anderson & Minster (1980*b*) rejected this mechanism as a candidate for seismic attenuation. For geometrical jogs, a lower bound for τ is obtained by taking $\lambda = 4\pi b$ and using the diffusivity of oxygen. Then $\tau \approx 5 \times 10^5$ s at 1600 K and 10 bar. Using silicon diffusivity and/or taking the effect of pressure into account can easily increase this value by several orders of magnitude. We may conclude that this mechanism might be a candidate for the attenuation of the Chandler wobble, although it is not clear that the anelastic theory of §2 still applies when the retardation times become comparable to the Maxwell time for steady-state creep.

(iv) *Dragging of point defects*

Dragging of an atmosphere of point defects bound to the dislocation is a more versatile and successful model. Original applications to internal friction are due to Weertman (1955), and Friedel *et al.* (1955). A specific model was proposed by Schoeck (1963) to explain the cold work peak in b.c.c. metals. Further improvements and modifications were subsequently proposed by Barrand & Leak (1964), Gibala (1967), Ino & Sugeno (1967), and more recently by Miner *et al.* (1976). Covalent crystals were considered by Southgate & Mendelson (1965). Dragging of a Cottrell atmosphere is an essential ingredient of Takeuchi & Argon's (1976*b*) model for steady-state creep. Binding of these defects to the dislocation line is usually assumed to be elastic, although electrical interaction probably is important in ionic crystals at high temperature (Eshelby *et al.* 1958; Brown 1961; Menezes & Nix 1974*a*, *b*).

This class of models has been demonstrably successful in the case of simple crystal structures. We propose to extend it to mantle materials. The point defects that contribute to drag may

include self-interstitials, impurity interstitials, or substitutional atoms with a slightly different ionic radius if the binding mechanism to dislocations is elastic.

Defects associated with a local charge imbalance (Smyth & Stocker 1975; Stocker & Smyth 1978; Stocker 1978) might be involved if electrical interaction is important. Let E_b be the binding energy of the point defect to the dislocation, and c_1 the bulk (lattice) concentration of defects away from dislocations. Then a very simple model of equilibrium between bound and unbound defects is obtained under the assumption that Fermi–Dirac statistics are applicable (Hirth & Lothe 1968). The high-temperature approximation yields a mean distance between defects along the core (see, for example, Miner *et al.* 1976)

$$\lambda \sim (b/c_1) \exp(-E_b/kT), \tag{88}$$

where binding energy is of the order of a few kcal/mol for many metals (see, for example, Nowick & Berry 1972). But the analysis leading to (88) assumes implicitly very pure material. This might be appropriate for intragrain environments if most impurities eventually migrate to grain boundaries as we have argued before (Anderson & Minster 1980*b*). On the other hand, if the binding energy is only 1 eV, then the exponential is of order 10^{-3} at mantle temperatures, and is thus of the same order or smaller than c_1. The high-temperature approximation (88) is no longer valid in that case, and we must consider the case where a very large fraction of core sites are occupied by a dragging point defect. The scale length λ is then comparable to b, and this limit yields an upper bound for τ.

Under these circumstances both D_{0Q} and E_Q^* are effective quantities for the diffusion of defects bound to the dislocation core. At sufficiently high temperatures, where (86) holds, E_Q^* would be augmented by the binding energy. In the absence of a good theory we shall ignore such complications. Potentially relevant diffusivity data include the cationic diffusion parameters in oxides, silicates and aluminates compiled by Ahrens & Schubert (1975), and a larger data set for metal oxides compiled by Kofstad (1972). If we restrict our attention to measurements involving a broad range of high temperatures, typical pre-exponential diffusivities are in the range 10^{-3}–10^{-2} cm^2/s, although order-of-magnitude fluctuations are not uncommon. For a tectonic stress of 10 bar, this implies a pre-exponential retardation time $\tau_0 \approx 10^{-6}$–10^{-5} s. If $\lambda > b$ this estimate should be lower. If we choose $\tau_0 = 10^{-6}$ s, then to bring the absorption band into the seismic range (1–10^3 s) at 1600 K, we require $45 \lesssim E_Q^* \lesssim 65$ kcal/mol. An increase of λ to $10^3 b$ changes this requirement to $65 \lesssim E_Q^* \lesssim 90$ kcal/mol. These values must be lowered if we choose a lower reference temperature, or if a lower tectonic stress is assumed. The permissible range encompasses the scatter of activation energies listed by Ahrens & Schubert (1975). It includes the range of estimates of 47–58 kcal/mol for interdiffusion of Mg^{2+} and Fe^{2+} in olivine (Misener 1974).

Unfortunately, there is little experimental evidence available to further constrain the class of acceptable models. Jackson (1969) found $\tau_0 \approx 4 \times 10^{-13}$ s and $E^* \approx 57$ kcal/mol for an absorption peak near 1 Hz in fine-grained olivine. He interpreted it as a grain boundary peak. However, we are interested in larger grain sizes, and higher temperatures, and therefore in the high-temperature background attenuation seen in Jackson's (1969) data, for which estimation of the relaxation parameters is difficult (Anderson & Minster 1980*b*).

Berckhemmer *et al.* (1979) used linearity to interpret transient creep superposed on a steady-state régime, in natural peridotites, in terms of attenuation $Q(\omega)$. However, the transient stress and steady-state load used were both in the 1–10^2 bar range; it is not clear whether the super-

position of transient and steady-state creep can be handled as we have done in our model, since the time scales and stress ranges tend not to be so clearly separated. The authors report an apparent activation energy of 30 kcal/mol for $Q(\omega)$, which they interpret as αE_s^* with $\alpha \sim 0.3$ (see, for example, Anderson & Minster 1980*a*). If instead we choose to interpret this number as E_Q^*, it falls on the low activation energy side of the bulk of cationic diffusion data. This, however, would be inconsistent with the observed frequency dependent, i.e. $(\omega\tau)^\alpha$, variation of Q in these experiments.

Although we do not have enough experimental constraints at our disposal to propose a better-specified model and then test it against geophysical data, we can still use seismological observations to limit the range of permissible models.

(*e*) *Absorption band in the mantle*

The model affords enough parameters (including tectonic stress σ_t), which may all vary with position, that there can be no doubt that all available geophysical observations could be explained by it. For illustration we shall only consider here the trade-offs between temperature, pressure, and tectonic stress, and consider other parameters to be fixed. In particular, we assume a low purity for mantle material, so that $\lambda \approx b$ and $\tau_0 \approx 10^{-6}$ s at $\sigma_t = 10$ bar and $T \approx 1500$ K.

At any given point in the mantle, the width of the band is then only controlled by the spectrum of activation energies. Since the strength Δ is fixed to be *ca.* 10 % in this model, the intensity of the absorption band (in the case $\alpha = 0$, equation (37)) is given by

$$Q_m \sim \frac{2}{\pi\Delta}\frac{\delta E^*}{RT}, \tag{89}$$

where δE^* is the range of activation energies. Several authors have argued that a low value of Q_m is required by seismic observations, at least in the regions of the mantle where the absorption band coincides with the seismic band. A value $Q_m \approx 25$ is in good agreement with the seismic data (Solomon 1972; Anderson & Hart 1978). Sipkin & Jordan (1979) report a $Q(\mathrm{ScS}) \approx 170$ for periods of 10–1000 s. If ScS should spend only one fourth of its travel time in the low Q regions of the Earth, then $Q_m \lesssim 40$. Equation (89) allows us to place a limit on the range of activation energies: at mantle temperatures $\delta E^* \lesssim \frac{1}{2}Q_m$ (kcal/mol). A range $45 \lesssim E^* \lesssim 60$ kcal/mol is therefore consistent with this constraint and with the laboratory data on cationic diffusion. Note that this yields an absorption band which is only about two decades wide at mantle temperatures. One consequence is that the value of α in (11) is rather immaterial, so that we will choose $\alpha = 0$.

For a temperature of 1500 K the range of retardation times is 3–500 s, which lies within the seismic band. An increase of temperature shifts the absorption band to higher frequencies; an increase in pressure has the opposite effect and so does a decrease in tectonic stress. Based on their observation that $Q(\mathrm{ScS})$ increases with frequency in the range 0.1–1 Hz, Sipkin & Jordan (1979) suggest an effective cut-off τ_m for the mantle absorption band averaged by ScS, near one second. Comparable conclusions have been reached by other investigators (for example, Kanamori & Anderson 1977; Minster 1978*b*; Lundquist 1979). In terms of our model, a high value for $Q(\mathrm{ScS})$ in the 1 Hz band means that this frequency does not lie within the frequency band for an extensive range of depths. The much lower values of $Q(\mathrm{ScS})$ reported by Sipkin & Jordan (1979) in the 10–1000 s band suggest in fact that the absorption band remains at periods longer than 1 s in spite of increasing temperature with depth.

PHILOSOPHICAL TRANSACTIONS OF THE ROYAL SOCIETY A MATHEMATICAL, PHYSICAL & ENGINEERING SCIENCES

This may be due either to a decrease in tectonic stress at depth, or to the effect of pressure if the activation volume is large enough. For example, a change of one order of magnitude in σ_t shifts the band by two decades in frequency. With an activation energy of *ca.* 50 kcal/mol and at mantle temperatures, a similar shift is achieved by a temperature change of about 400 °C. Thus it may be expected that the stress–temperature trade-off is most important in regions with a high geothermal gradient and a simultaneous decrease of stress with depth, such as the upper mantle (see, for example, Schubert *et al.* 1976). On the other hand, if dynamical transition zones (boundary layers) mark the bottom of convection cells in the mantle (Jeanloz & Richter 1979) then both temperature and stress increases would tend to combine and cause a rapid shift of the absorption band toward higher frequencies. This might provide a physical interpretation for a low Q zone of the sort hypothesized by Anderson & Hart (1978) at the base of the mantle.

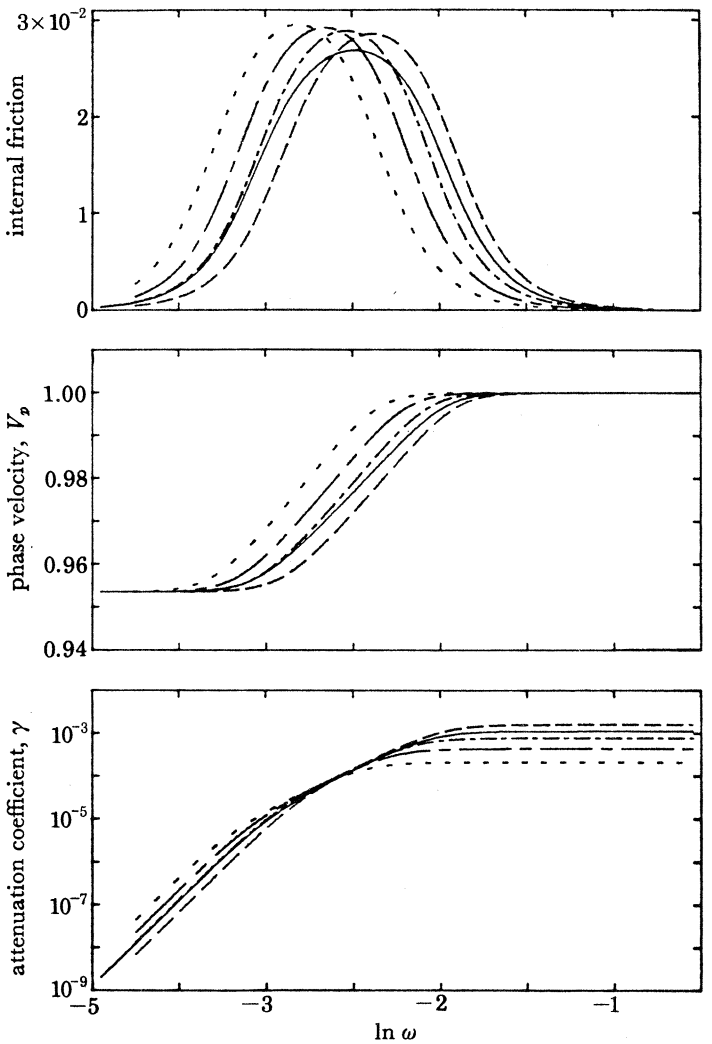

FIGURE 10. Hypothesized mantle absorption band for $\Delta = 10\,\%$, $\sigma_t = 10$ bar, $45 \leqslant E_Q^* \leqslant 60$ kcal/mol. $V_Q^* = 4$ cm³/mol, calculated at pressures of 100–500 kbar, for which indicated temperatures were assumed, Also shown are the dispersive properties associated with the absorption band. T/K: - - -, 1730; ——— – ———, 1700; – – – –, 1670; – – – –, 1640; ——, 1500.

Discussion of the effect of pressure is predicated on the adoption of an activation volume V_Q^*, for which we have no data. For purposes of discussion, let us consider again a geotherm with a linear 0.3 K/km gradient and a temperature of 1700 K at 400 km depth. For a pressure-independent activation volume V_Q^*, and at constant tectonic stress σ_t, the effect of pressure will overcome the effect of temperature if

$$\frac{\mathrm{d}}{\mathrm{d}P}\left(\frac{E_Q^*+PV_Q^*}{RT}\right) \geqslant 0, \tag{90}$$

or

$$V_Q^* \gtrsim 2.5\times 10^{-2}E_Q^*, \tag{91}$$

where V_Q^* is in cm³/mol and E_Q^* is in kcal/mol. Thus, with a spectrum of activation energies between 45 and 60 kcal/mol, and the geotherm described above, the absorption band shifts to longer period with increasing depth if $V_Q^* \gtrsim 1.1$ cm³/mol. To illustrate this phenomenon

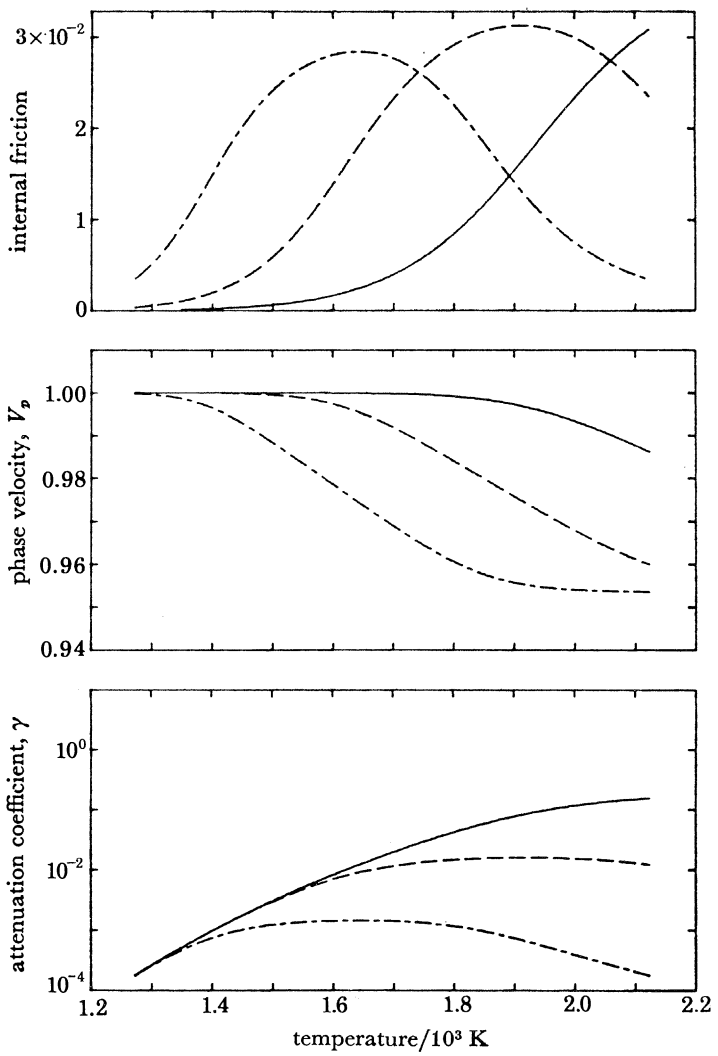

FIGURE 11. Temperature dependence of absorption band of figure 10, for three frequencies appropriate for laboratory experiments, indicating possible interpretation in terms of high-temperature background attenuation. – · – · –, $\omega = 0.1$; – – –, $\omega = 1$; ——, $\omega = 10$.

PHILOSOPHICAL TRANSACTIONS OF THE ROYAL SOCIETY A MATHEMATICAL, PHYSICAL & ENGINEERING SCIENCES

we show in figure 10 the absorption band and associated dispersion, for a fixed stress $\sigma_t = 10$ bars, at depths of 100, 200, ..., 500 km, for which the assumed temperatures are indicated in the figure legend. V_Q^* was fixed at 4 cm³/mol, a value large enough to illustrate the initial shift of the band to high frequency with rapidly increasing temperature, followed by a progressive shift toward longer periods, owing to increased pressure.

More complicated scenarios can of course be envisaged, with a spectrum of activation volumes, phase transitions, etc. Some of these refinements have been considered by Lundquist (1979, 1980). They go well beyond our present purposes.

(*f*) *High-temperature background attenuation* (*h.t.b.*)

We have suggested before (see, for example, Anderson & Minster 1980*b*) that the dominant mechanism of attenuation in the mantle corresponds to the h.t.b. in laboratory experiments. A description of its properties is found in Nowick & Berry (1972). An important, unanswered, question is whether the h.t.b. is anelastic or viscoelastic in nature. The work of Friedel *et al.* (1955), and more recently the analysis of Woirgard (1976), clearly indicate the possibility of a broad, high-temperature anelastic peak. Figure 11 shows our model at zero pressure and at frequencies comparable to laboratory experiments. It points to a testable aspect of the model, namely the development of a peak, at sufficiently low frequency and/or high temperature. Observation of such a peak, in well annealed material deformed under low stress to steady state, would not only either provide support for our model or infirm it, but it would yield needed direct estimates of the model parameters.

5. Conclusions

The main conclusion of this work is that a dislocation microstructure model is capable of simultaneously explaining steady-state creep and attenuation in the mantle. Our preferred model involves a sharply organized microstructure, where most dislocations are found in cell walls. Steady-state creep is controlled by recovery through climb in the cell walls. Good quantitative agreement with laboratory observations of creep in olivine is obtained if silicon controls self-diffusion. However, because of the larger activation volume of oxygen, we expect that oxygen diffusion will become the controlling factor at sufficient depth. We hypothesize that the discrepancy between oxygen or silicon diffusion activation energies and the observed activation energy for creep is a measure of jog formation energy, which is then somewhat greater than 35 kcal/mol, depending on the efficiency of core diffusion.

Attenuation of seismic waves takes place through bowing of the few intracell dislocations, controlled either by kink diffusion (particularly at high frequency) or by the dragging of an atmosphere of point defects bound to the dislocations. Owing to the paucity of laboratory observations, the success of this model is judged on more qualitative and circumstantial evidence.

The microstructure depends on the long-term tectonic stress, which exerts a strong influence on both creep and attenuation properties. Within the framework of this model, stress, viscosity and Q are related, so that estimating one of these parameters provides constraints on the others. The scaling laws do not favour a wide spread of length scales, so that the relaxation strength is fixed in this model, and is of the order of 10 %. A broad absorption band can be achieved with a spectrum of activation energies, but seismological requirements as to the intensity of attenuation in the band limit its width to 2–3 decades. The main parameters controlling the

PHILOSOPHICAL TRANSACTIONS OF THE ROYAL SOCIETY A MATHEMATICAL, PHYSICAL & ENGINEERING SCIENCES

position of the low-Q band are temperature, pressure, and tectonic stress. The absorption band coincides with the seismic band in the upper mantle, but shifts to longer periods at greater depths owing to the combined effects of increased pressure and possibly decreased shear stress. It must be noted, however, that sharp shifts to shorter periods are expected in hypothetical boundary layers, owing to larger temperature gradients and higher stresses. In the bulk of the mantle, however, seismic frequencies appear to be on the high-frequency, low-temperature side of the absorption band. The absorption band can also be expected to be broadened in the mantle because of the distributions in D_0, E^*, l and μ expected for a polymineralic aggregate, and the anisotropy of the grains. Each mineral has its own physical properties but, at least in the upper mantle, the total breadth of the band is constrained by the minimum allowable damping.

Our models adopt a very simple view of dislocations in complex crystal structures pertinent to silicates. We have ignored the complications associated with partial dislocations, and the differences between dislocations with different Burgers vectors. A more detailed discussion is provided, for example, by Gueguen (1979) (see also the comment by Poirier at the end of Goetze's (1978) paper). The dislocation model proposed here may be viewed as a possible alternative to grain boundary mechanisms described, for example, by O'Connell & Budiansky (1977). Its validity must be ultimately tested against further experimental data.

This research was supported by the Earth Sciences Section National Science Foundation grant no. EAR77-14675, and National Aeronautics and Space Administration grant no. NSG-7610.

References

Ahrens, T. J. & Schubert, G. 1975 Gabbro-eclogite reaction rate and its geophysical significance. *Rev. Geophys. Space Phys.* **13**, 383–400.

Anderson, D. L. 1966 Earth's viscosity. *Science, Wash.* **151**, 321–322.

Anderson, D. L. & Hart, R. S. 1978 Attenuation models of the earth. *Physics Earth planet. Inter.* **16**, 289–306.

Anderson, D. L., Kanamori, H., Hart, R. S. & Liu, H. P. 1976 The Earth as a seismic absorption band. *Science, Wash.* **196**, 1104–1106.

Anderson, D. L. & Minster, J. B. 1980*a* Seismic velocity, attenuation and rheology of the upper mantle. In *Source mechanism and earthquake prediction* (Coulomb volume, C. J. Allègre ed.) pp. 13–22. Paris: C.N.R.S.

Anderson, D. L. & Minster, J. B. 1980*b* The physics of creep and attenuation in the mantle. (Submitted.)

Ashby, M. F. & Verall, R. A. 1978 Micromechanisms in flow and fracture, and their relevance to the rheology of the upper mantle. *Phil. Trans. R. Soc. Lond.* A **288**, 59–95.

Barrand, P. & Leak, C. M. 1964 Precipitation and the deformation damping peak in iron alloys. *Acta metall.* **12**, 1147–1152.

Berckhemmer, H., Auer, F. & Drisler, J. 1979 High-temperature anelasticity and elasticity of mantle peridotite. *Physics Earth planet. Inter.* **20**, 48–59.

Brown, L. M. 1961 Mobile charged dislocations in ionic crystals. *Physica Status Solidi*, **1**, 585–599.

Crough, S. T. 1977 Isostatic rebound and power-law flow in the asthenosphere. *Geophys. Jl R. astr. Soc.* **50**, 723–738.

Durham, W. B. & Goetze, C. 1977 Plastic flow of oriented single crystals of olivine. I. Mechanical data. *J. geophys. Res.* **82**, 5737–5754.

Durham, W. B., Goetze, C. & Blake, B. 1977 Plastic flow of oriented single crystals of olivine. II. Observations and interpretations of the dislocation structures. *J. geophys. Res.* **82**, 5755–5770.

Eshelby, J. D., Newey, C. W. A., Pratt, P. L. & Lidiard, A. B. 1958 Charged dislocations and the strength of ionic crystals. *Phil. Mag.* **3**, 75–89.

Friedel, J. 1964 *Dislocations*, p. 491. New York: Pergamon Press.

Friedel, J., Boulanger, C. & Crussard, C. 1955 Constantes élastiques et frottement intérieur de l'aluminium polygonisé. *Acta metall.* **3**, 380–391.

Gibala, R. 1967 On the mechanism of the Köster relaxation peak. *Acta metall.* **15**, 428–430.

Gittus, J. H. 1976*a* Theoretical equation for steady-state dislocation creep effects of jog drag and cell formation. *Phil. Mag.* **34**, 401–411.

PHILOSOPHICAL TRANSACTIONS OF THE ROYAL SOCIETY A MATHEMATICAL, PHYSICAL & ENGINEERING SCIENCES

Gittus, J. H. 1976*b* Theoretical value of the ratio (K) of cell diameter to dislocation spacing for a material undergoing dislocation creep. *Phil. Mag.* **35**, 293–300.
Goetze, C. 1978 The mechanisms of creep in olivine. *Phil. Trans. R. Soc. Lond.* A **288**, 99–119.
Goetze, C. & Brace, W. F. 1972 Laboratory observations of high temperature rheology of rocks. *Tectonophysics* **12**, 583–600.
Goetze, C. & Kohlstedt, D. L. 1973 Laboratory study of dislocation climb and diffusion in olivine. *J. geophys. Res.* **78**, 5961–5971.
Granato, A. & Lücke, K. 1956 Theory of mechanical damping due to disclocations. *J. appl. Phys.* **27**, 583–593.
Green, H. W. & Radcliffe, S. V. 1972 Dislocation mechanisms in olivine and flow in the upper mantle. *Earth planet. Sci. Lett.* **15**, 239–247.
Gueguen, Y. 1979 High temperature olivine creep: evidence for control by edge dislocations. *Geophys. Res. Lett.* **6**, 357–360.
Gueguen, Y. & Mercier, J. M. 1973 High attenuation and the low-velocity zone. *Physics Earth planet. Inter.* **7**, 39–46.
Hirth, J. & Lothe, J. 1968 *Theory of dislocations*, p. 780. New York: McGraw-Hill.
Holt, D. L. 1970 Dislocation cell formation in metals. *J. appl. Phys.* **41**, 3197–3201.
Ino, H. & Sugeno, T. 1967 The cold-work damping peak in Alpha-iron. *Acta metall.* **15**, 1197–1205.
Jackson, D. 1969 Grain boundary relaxation and the attenuation of seismic waves. Ph.D. thesis, M.I.T., Cambridge, Massachusetts.
Jaoul, O., Froideveaux, C. & Poumellec, M. 1979 Atomic diffusion of ^{18}O and ^{30}Si in forsterite: implication for the high temperature creep mechanism. Abstract, I.U.G.G. XVII General Assembly, Canberra, Australia.
Jeanloz, R. & Richter, F. M. 1979 Convection, composition, and the thermal state of the lower mantle. *J. geophys. Res.* **89**, 5497–5504.
Jeffreys, Sir Harold 1970 *The Earth*, 5th edn. London: Cambridge University Press.
Jeffreys, H. & Crampin, S. 1970 On the modified Lommitz law of damping. *Mon. Not. R. astr. Soc.* **147**, 295–301.
Kanamori, H. & Anderson, D. L. 1977 Importance of physical dispersion in surface-wave and free-oscillation problems, review. *Rev. Geophys. Space Phys.* **15**, 105–112.
Koehler, J. S. 1952 *Imperfections in nearly perfect crystals*. New York: Wiley.
Kofstad, P. 1972 *Nonstoichiometry, diffusion, and electrical conductivity in binary metal oxides*, p. 382. New York: Wiley–Interscience.
Kohlstedt, D. L. 1979 Creep behavior of mantle materials. Abstract; I.U.G.G. XVII General Assembly, Canberra, Australia.
Kohlstedt, D. L. & Goetze, C. 1974 Low-stress high-temperature creep in olivine single crystals. *J. geophys. Res.* **79**, 2045–2051.
Liu, H. P., Anderson, D. L. & Kanamori, H. 1976 Velocity dispersion due to anelasticity; implications for seismology and mantle composition. *Geophys. Jl R. astr. Soc.* **47**, 41–58.
Lundquist, G. M. 1979 The frequency dependence of Q. Ph.D. thesis, CIRES, University of Colorado, Boulder, Colorado.
Lundquist, G. M. 1980 Constraints on the absorption band model of Q. *J. geophys. Res.* (Submitted.)
Macdonald, J. R. 1961 Theory and application of a superposition model of internal friction and creep. *J. appl. Phys.* **3**, 2385–2398.
Macdonald, J. R. 1963 Transient and temperature response of a distributed thermally activated system. *J. appl. Phys.* **34**, 538–552.
Meissner, R. & Vetter, U. 1979 Relation between the seismic quality factor Q and the effective viscosity. *J. geophys. Res.* **45**, 147–158.
Menezes, R. A. & Nix, W. D. 1974*a* High temperature dislocation mobility in LiF. I. Charged dislocations in ionic crystals. *Mater. Sci. Engng* **16**, 57–66.
Menezes, R. A. & Nix, W. D. 1974*b* High temperature dislocation mobility in LiF. II. Glide mobility of dislocations at high temperatures. *Mater. Sci. Engng* **16**, 67–73.
Miner, R. E., Gibala, R. & Hultgren, F. A. 1976 An application of the Schoeck theory to the cold-work internal friction peak in iron. *Acta metall.* **24**, 233–239.
Minster, J. B. 1978*a* Transient and impulse responses of a one-dimensional linearly attenuating medium. I. Analytical results. *Geophys. Jl R. astr. Soc.* **52**, 479–502.
Minster, J. B. 1978*b* Transient and impulse responses of a one-dimensional linearly attenuating medium. II. A parametric study. *Geophys. Jl R. astr. Soc.* **52**, 503–524.
Minster, J. B. 1980 Anelasticity and attenuation. In *Proc. Enrico Fermi int. School Physics* (ed. A. Dziewonski & E. Boschi). New York: Academic Press.
Minster, J. B. & Anderson, D. L. 1980 Dislocations and nonelastic processes in the mantle. *J. geophys. Res.* **85**, 6347–6352.
Misener, D. V. 1974 Cationic diffusion in olivine to 1400 °C and 35 kbar. *Carnegie Instn. Wash. Publs.* **634**, 117–129.
Mukherjee, A. K., Bird, J. E. & Dorn, J. E. 1969 Experimental correlations for high-temperature creep. *A.S.M. Trans.* **62**, 155–179.
Nowick, A. & Berry, B. 1972 *Anelastic relaxation in crystalline solids*, p. 677. New York: Academic Press.

PHILOSOPHICAL TRANSACTIONS OF THE ROYAL SOCIETY A MATHEMATICAL, PHYSICAL & ENGINEERING SCIENCES

Nur, A. & Mavko, G. 1974 Postseismic viscoelastic rebound. *Science, Wash.* **183**, 204–206.
O'Connell, R. J. 1977 On the scale of mantle convection. *Tectonophysics.* **38**, 119–136.
O'Connell, R. J. & Budiansky, B. 1977 Viscoelastic properties of fluid-saturated cracked solids. *J. geophys. Res.* **82**, 5719–5736.
O'Connell, R. J. & Budiansky, B. 1978 Measures of dissipation in viscoelastic media. *Geophys. Res. Lett.* **5**, 5–8.
Peltier, W. R. 1980 Mantle convection and viscosity. In *Proc. Enrico Fermi Int. School Physics* (ed. A. Dziewonski & E. Boschi). New York: Academic Press.
Poirier, J. P. 1976 *Plasticité à haute température des solides cristallins.* Paris: Eyrolles.
Poumellec, M., Jaoul, O., Froidevaux, C. & Havette, A. 1980 Silicon diffusion in forsterite: A new constraint for understanding mantle deformation. (Preprint.)
Raleigh, C. B. & Kirby, S. H. 1970 Creep in the upper mantle. *Mineralog. Soc. Am. Spec. Pap.* **3**, 113–121.
Reddy, K. P. R., Oh, S. M., Major, L. D. Jr. & Cooper, A. R. 1980 Oxygen diffusion in forsterite. *J. geophys. Res.* **85**, 322–326.
Sammis, C. G., Smith, J. C., Schubert, G. & Yuen, D. A. 1977 Viscosity–depth profile of the Earth's mantle: effects of polymorphic phase transitions. *J. geophys. Res.* **82**, 3747–3761.
Schoeck, G. 1963 Fricción interna debido a la interacción entre dislocaciones y atomos solutos. *Acta metall.* **11**, 617–622.
Schubert, G., Froidevaux, C. & Yuen, D. A. 1976 Oceanic lithosphere and asthenosphere: thermal and mechanical structure. *J. geophys. Res.* **81**, 3525–3540.
Schwenn, M. & Goetze, C. 1978 Creep of olivine during hot-pressing. *Tectonophysics* **48**, 41–60.
Simpson, H. M. & Sosin, A. 1972 Contribution of defect dragging to dislocation damping. I. Theory. *Phys. Rev.* B **5**, 1382–1393.
Sipkin, S. & Jordan, T. 1979 Frequency dependence of Q_{88}. *Bull. seism. Soc. Am.* **69**, 1055–1079.
Smyth, D. M. & Stocker, R. L. 1975 Point defects and non-stoichiometry in forsterite. *Phys. Earth Planet. Int.* **10**, 183–192.
Solomon, S. C. 1972 On Q and seismic discrimination. *Geophys. Jl R. astr. Soc.* **31**, 163–177.
Southgate, P. D. & Mendelson, K. S. 1965 High-temperature dislocation damping in covalent crystals. *J. appl. Phys.* **36**, 2685–2692.
Stocker, R. L. 1978 Influence of oxygen pressure on defect concentrations in olivine with a fixed cationic ratio. *Physics Earth planet. Inter.* **17**, 118–129.
Stocker, R. L. & Ashby, M. F. 1973 On the rheology of the upper mantle. *Rev. Geophys. Space Phys.* **11**, 391–497.
Stocker, R. L. & Smyth, D. M. 1978 Effect of enstatite activity and oxygen partial pressure on the point-defect chemistry of olivine. *Physics Earth planet. Inter.* **16**, 145–156.
Strick, E. 1970 A predicted pedestal effect for pulse propagation in constant-Q solids. *Geophys.* **35**, 387–403.
Takeuchi, S. & Argon, A. S. 1976*a* Steady-state creep of single-phase crystalline matter at high temperature. *J. Mater. Sci.* **11**, 1542–1566.
Takeuchi, S. & Argon, A. S. 1976*b* Steady-state creep of alloys due to viscous motion of dislocations. *Acta metall.* **24**, 883–890.
Weertman, J. 1955 Internal friction of metal single crystals. *J. appl. Phys.* **26**, 202–210.
Weertman, J. 1970 The creep strength of the Earth's mantle. *Rev. Geophys. Space Phys.* **8**, 145–168.
Weertman, J. 1975 High temperature creep produced by dislocation motion. J. E. Dorn Memorial Symposium, Cleveland, Ohio, published in *Processes in Plastic Deformation of Materials*, American Society of Metals, pp. 315–336.
Woirgard, J. 1976 Modèle pour les pics de frottement interne observés à haute température sur les monocristaux. *Phil. Mag.* **33**, 623–637.

PHILOSOPHICAL TRANSACTIONS OF THE ROYAL SOCIETY A MATHEMATICAL, PHYSICAL & ENGINEERING SCIENCES